THE ASTRONOMICAL JOURNAL VOLUME 111, NUMBER 3 MARCH 1996

MEMBERSHIP OF STARS IN NGC 1039 (M34)[1]

B. F. Jones and Charles F. Prosser[2]

University of California Observatories/Lick Observatory, Board of Studies in Astronomy and Astrophysics, University of California, Santa Cruz, California 95064

Electronic mail: jones@ucolick.org, prosser@cfa0.harvard.edu

Received 1995 September 20; revised 1995 December 8

ABSTRACT

We have measured proper motions, positions, magnitudes, and colors for 630 stars to $V \sim 16.2$ in the vicinity of the open cluster NGC 1039=M34. A proper motion membership probability analysis has been performed. We give for all stars the equatorial coordinates, the proper motions, the V magnitude, and the membership probability. For the most likely cluster members we also give $B-V$ and $(V-I)_K$ colors. Cross identifications with previous surveys are also provided. We find an age for the cluster of 200–250 Myr and a distance of 475 parsecs. © *1996 American Astronomical Society.*

1. INTRODUCTION

The open cluster NGC 1039 (M34, 1950 coordinates $2^h38\overset{m}{.}9$, $+42°34'$) has the potential of being an important cluster for the study of the evolution of rotational velocity, chromospheric activity, and lithium abundance in solar type stars. At an age of ~200 Myr (Meynet *et al.* 1993), M34 is midway in age between the younger Pleiades (~70 Myr) and the older Hyades (~800 Myr), two of the best studied open clusters in the sky. Although significantly further away than either the Pleiades or the Hyades, M34 is still close enough (~450 pc, Ianna & Schlemmer 1993, hereinafter referred to as IS) that stars slightly less massive than the sun can be observed at high dispersion with a good Coude spectrograph on a large telescope.

There have been several previous proper motion studies of this cluster. Brüggemann (1937) measured positions and proper motions for 190 stars, mostly brighter than $m_{pg}=13$, in the region of the cluster. Dieckvoss (1954) published tangential coordinates for 492 stars in the vicinity of the cluster and proper motions for 97. Latypov (1973) measured proper motions for 696 stars within ~1/2° of the cluster center. More recently, IS determined proper motions and membership probabilities for 354 stars to a limiting magnitude slightly fainter than visual magnitude 14.

Because stars of interest for rotation and lithium abundance extend to a fainter limiting magnitude than the IS study, we decided to do another proper study of this cluster using plates available at Lick and Yerkes observatories.

2. DATA REDUCTION

2.1 Proper Motions

The plates we had available for measurement are listed in Table 1. Those with prefix LC were taken with the Lick 36 in. refractor, while the others were taken with the Yerkes 40 in. refractor. The Lick plates were taken on 103a-G emulsion behind an OG-4 filter. The Yerkes plates with prefix F were taken on I-G emulsion behind a Shott GG7 filter, while those with prefix π were taken on II-G emulsion behind a GG14 filter. The plates had very different exposure times, and hence very different limiting magnitudes.

One of the deep plates was surveyed manually on the Lick Gaertner Survey Machine, and a master list of rough coordinates for 741 stars within 17′ of the plate center was produced. This list contained all stars from the brightest to the plate limiting magnitude. The brighter stars on this list were too overexposed to be measured on the long exposure plates, while the fainter stars did not appear on the shorter exposure plates. Two lists of input coordinates for measurement were produced from the master list, one of brighter stars for measuring the short exposure plates and one of fainter stars for measuring the longer exposure plates. The two lists had a large overlap in the V magnitude range 11.8–14.0.

All the exposure systems on all the plates were measured in both direct and reverse orientation on the Lick Gaertner Automatic Measuring Engine (AME; Klemola *et al.* 1987), using the appropriate set of input coordinates. The AME produces accurate x,y coordinates as well as a photometric reading that measures the density of the stellar images. After measurement, the measures were inspected as a function of photometer reading and stars too bright or too faint were rejected. The direct and reverse measures were compared, and mismeasurements rejected. The direct and reverse measures were then combined.

Proper motions were computed using an iterative central overlap algorithm long in use at Lick Observatory (Jones & Walker 1988). Briefly, one plate was used as a reference plate, and the measures on all other plates were reduced against this plate, with the option of using a wide variety of plate reduction models. The residuals for each star on each plate from this *plate constant* solution were then used to compute preliminary proper motions for each star. For the second iteration, these preliminary proper motions were used to select reference stars near the centroid of the cluster mo-

[1]Lick Observatory Bulletin No. 1328.
[2]Currently at Harvard-Smithsonian Center for Astrophysics.

TABLE 1. Plates.

Plate	Epoch (1900+)	Exp (min)	Plate	Epoch (1900+)	Exp (min)
F 501	38.12	25	LC 8139	90.78	60
F 579	38.12	52	LC 8140	90.78	15
F 594	38.96	12, 7	LC 8141	90.78	15
F 595	39.02	20, 15	LC 8142	90.78	5
π 21308	59.93	20	LC 8143	90.78	5
π 21369	64.06	10	LC 8144	90.78	60
LC 7711	77.73	60	LC 8145	90.78	5
LC 7712	77.73	60	LC 8146	90.78	5
LC 7713	77.73	5	LC 8147	90.78	60
LC 7877	79.69	60	LC 8148	90.78	15
LC 7886	79.69	120	LC 8149	90.78	15
LC 8138	90.78	7			

tion in the proper motion vector point diagram. Using these reference stars, the transformation from each plate to the reference plate was redetermined, and the residuals used to compute new proper motions and mean positions at the epoch of the reference plate. For the third and following iterations, all plates were reduced against the mean positions using all measured stars, using the proper motions to update the measured positions on each plate to the epoch of the reference plate, and using the residuals from these plate constant solutions to calculate corrections to the proper motions and mean positions. In general, four iterations brought convergence.

Because of the wide difference in the magnitude range that could be measured on the different plates, two sets of proper motion reductions were undertaken, one for the shorter exposure plates, and one for the longer exposure plates. There were 140 stars in common. For each set, initial reductions were done unweighted. Obvious mismeasurements not found earlier were thrown out. Subsequent reductions were done with a plate weight determined by the rms residuals on the initial reductions. Reductions for the plate constant solutions at first contained terms for scale, orientation, zero-point, and tangent-point differences. It quickly became apparent, however, that a significant magnitude term was needed for many of the plates, and the final model included the above terms plus a linear magnitude term. The method used above, when one has a significant number of cluster stars so as to allow the centroid of the cluster motion to be determined for each magnitude interval, insures that the introduction of a linear magnitude does not introduce systematic error.

The reductions for the bright stars and the faint stars were brought to the same system using the 140 stars common to both data sets. For the proper motions, this involved a simple zero-point correction, while for the positions, scale change, and orientation were also included. The mean differences in the proper motions between the two sets were $-0''.02$ and $0''.02$ cent^{-1} and the rms differences $0''.11$ and $0''.07$ cent^{-1} in x and y, respectively. The rms position differences were 1 μm for both x and y.

We have 190 stars in common with IS. We note that in IS there is a sign error in the both the y positions and proper

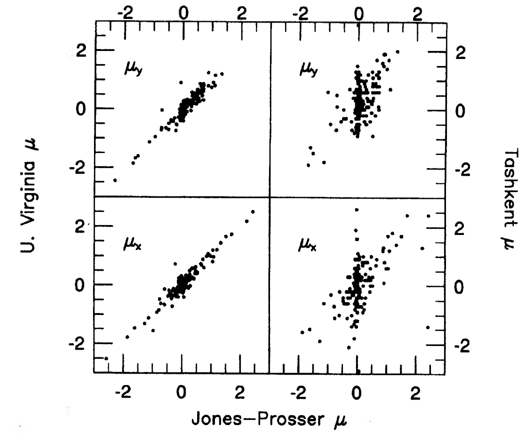

FIG. 1. A plot of the proper motions obtained here (Jones–Prosser) vs those measured by IS (U. Virginia, left panel) and those measured by Latypov (Tashkent, right panel). Units are arcseconds per century.

motions. The mean offsets (in the sense our proper motions minus the IS motions, and after changing the sign of the IS motions) are $\Delta\mu_x = -0''.05$ cent^{-1} and $\Delta\mu_y = 0''.02$ cent^{-1} with dispersions about the mean offset of $\sigma_x = 0''.16$ cent^{-1} and $\sigma_y = 0''.21$ cent^{-1}. We had 177 stars in common with the Tashkent proper motion study (Latypov 1973). The mean offsets (in the sense our proper motions minus the Tashkent motions) are $\Delta\mu_x = -0''.02$ cent^{-1} and $\Delta\mu_y = -0''.27$ cent^{-1} with dispersions about the mean offset of $\sigma_x = 0''.73$ cent^{-1} and $\sigma_y = 0''.59$ cent^{-1}. Figure 1 gives a graphical comparison between our motions and those of IS and Latypov.

2.2 Positions

We obtained equatorial coordinates for all program stars. We first set up a secondary reference in the vicinity of the cluster, using 20 AGK3 stars as the primary reference frame. To set up the secondary reference frame, the 20 AGK3 stars and a selection of 34 program stars were measured on a Lick Carnegie astrograph (scale $55''.1$ mm^{-1}) plate AY8091 (epoch 1975.75) taken for the Lick Northern Proper Motion Program (Klemola *et al.* 1987) and centered at 2^h48^m, $+40°$ (1950). The AGK3 proper motions were used to update the AGK3 positions to the epoch of the plate and standard coordinates computed using the nominal field center given above. The transformation between the measured positions and the standard coordinates was determined using a model that included terms for scale, orientation, zero-point, and tangent-point differences. The mean error for a position in this transformation was $0''.37$ in x and $0''.22$ in y, mainly due to proper motion and position errors in the AGK3. This transformation was then used to obtain equatorial coordinates for the 34 program stars.

The equatorial coordinates of the 34 program stars in the secondary reference frame and the mean x,y positions determined above were used to calculate standard coordinates using a nominal field center for the cluster of $2^h38^m48^s$, $+42°34'$ (1950). No proper motion correction was made because (1) the proper motions for our stars are not on the system of the AGK3 and (2) the epoch difference between the mean positions from the proper motion solution and the

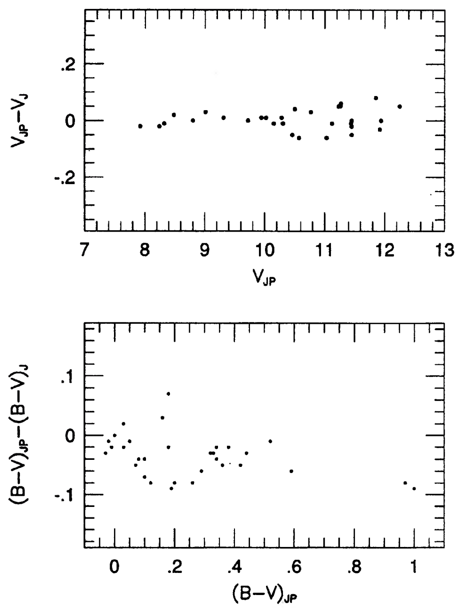

FIG. 2. A comparison of the photometry obtained here with that of Johnson (1954). The differences are in the sense our photometry minus Johnson's.

epoch of plate AY8091 (1.36 years) is small. The transformation between the measured positions and the standard coordinates were determined again using a model that included terms for scale, orientation, zero-point, and tangent-point differences. The mean error for a position in this transformation was 0$''$.08 in x and 0$''$.13 in y, mainly due to the accidental errors in the positions of the 34 secondary reference frame stars. This transformation was then used to obtain equatorial positions for all the program stars.

2.3 *Magnitudes and Colors*

Photometry of stars in the central region of the cluster was obtained on the nights of 1990 October 20 and October 30 UT using the 1 m Nickel telescope of Lick Observatory. Observations in B, V, and I bandpasses were obtained using a thinned TI 500×500 CCD at a scale of 0$''$.54 pixel^{-1}, giving a 4$'$.5×4$'$.5 field. The instrumental magnitudes were extinction corrected and then transformed to a B, V and I (Kron) system using transformation relations obtained from observations of standard stars on other nights with the same system, since, regrettably, insufficient standards were observed on the same nights as the M34 stars.

A comparison of the transformed magnitudes with the $(V,B-V)$ photometry of Johnson (1954) indicated an offset of 0.27 mag in V. Our photometry was shifted by this mean offset to agree with system of Johnson. A small offset of -0.03 in the $B-V$ color was not corrected for. The rms differences between our photometry and that of Johnson is 0.035 mag in V and 0.036 in $B-V$ after accounting for the zero-point differences. Figure 2 shows a comparison between Johnson's and our V and $B-V$. We made a comparison between our $B-V$ and $(V-I)_K$ colors, as discussed in Sec. 3.2 below. That comparison also gave a precision of 0.035 mag for $B-V$ and $(V-I)_K$. Thus we believe that our precision is

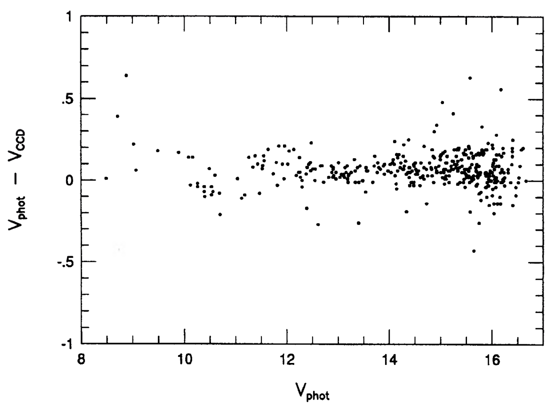

FIG. 3. A comparison of our CCD photometry and our photographic photometry.

about 0.035 mag. Of course, the systematic errors, especially for the fainter stars, could be much larger. Better photometry is obviously needed.

For stars without CCD photometry, photographic V magnitudes were available from our AME photometry of the astrometric plates using the CCD V magnitudes as standards. The rms difference between the photographic V and CCD V magnitudes was 0.14 mag. A comparison between our photographic and CCD magnitudes is shown in Fig. 3.

2.4 *Membership Probabilities*

Membership probabilities were determined using the methods developed at Lick. Since the methodology is described in detail in previous publications (Jones & Walker 1988; Francic 1989; Jones & Stauffer 1991), we just outline it here. Basically, the algorithm fits the density of points in the proper motion vector point diagram (vpd) using a model separately describing the density of field stars and cluster members, and simultaneously fits the areal density of field stars and cluster stars on the plane of the sky. For NGC 1039 we used a bivariate normal distribution to fit both cluster and field in the vpd, a constant density to fit the field areal density, and an exponential to fit the cluster areal density, the same as was done in Jones & Walker (1988). Let $\Phi(m,\mu_x,\mu_y,r)$ be the density of stars in the proper motion vector point diagram at μ_x,μ_y, at a projected distance r from the cluster center, and of magnitude m. Then

$$\Phi(m,\mu_x,\mu_y,r)=\Phi_f(m,\mu_x,\mu_y)+\Phi_c(m,\mu_x,\mu_y,r),$$

where Φ_f and Φ_c are the separate densities of field and cluster stars, respectively

$$\Phi_f=f_0(2\pi\Sigma_x\Sigma_y)^{-1}e^{-1/2[(\mu_x-\mu_{x,F}/\Sigma_x)^2+(\mu_y-\mu_{y,F}/\Sigma_y)^2]},$$

$$\Phi_c=\rho_0 e^{-r/r_0}(2\pi\sigma_x\sigma_y)^{-1}$$
$$\times e^{-1/2[(\mu_x-\mu_{x,c}/\sigma_x)^2+(\mu_y-\mu_{y,c}/\sigma_y)^2]},$$

where

σ_x=the cluster proper motion dispersion in x,
σ_y=the cluster proper motion dispersion in y,
Σ_x=the field proper motion dispersion in x,
Σ_y=the field proper motion dispersion in y,

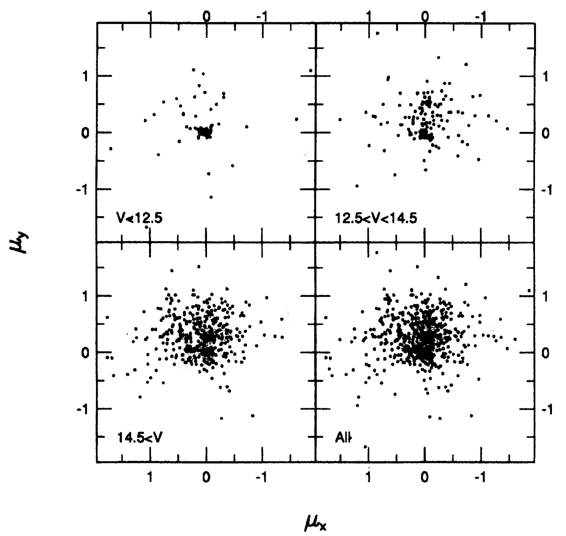

FIG. 4. Proper motion vector point diagrams for the magnitude groupings indicated. Units are arcseconds per century.

$\mu_{x,c}$=the mean cluster proper motion in x,
$\mu_{y,c}$=the mean cluster proper motion in y,
$\mu_{x,f}$=the mean field proper motion in x,
$\mu_{y,f}$=the mean field proper motion in y,
ρ_0=projected density of cluster stars at cluster center,
r_0=scale length for projected cluster density,
f_0=(constant) field star projected density.

ρ_0, r_0 and f_0 are not independent, since we know the total number of stars within our measuring area. Jones & Stauffer (1991) discuss the normalization of the areal density functions. As discussed in the above papers, the model fitting parameters listed above can be very magnitude dependent. This is illustrated in Fig. 4, which shows proper motion vector diagrams for three different magnitude groupings, as while as for the entire data set.

The parameters were determined using a maximum-likelihood technique (Sanders 1971) as modified by Francic (1989). Because of the dependence of the parameters on magnitude, we obtained solutions for these parameters by selecting stars in magnitude bins 2 mag wide, and moving the bin center 1/2 mag between solutions. This allowed us to determine the magnitude dependence of the parameters, as shown in Table 2. The units in Table 2 are arcminutes for r_0 and arcsec cent^{-1} for the other quantities.

The data in Table 2 were plotted against magnitude and

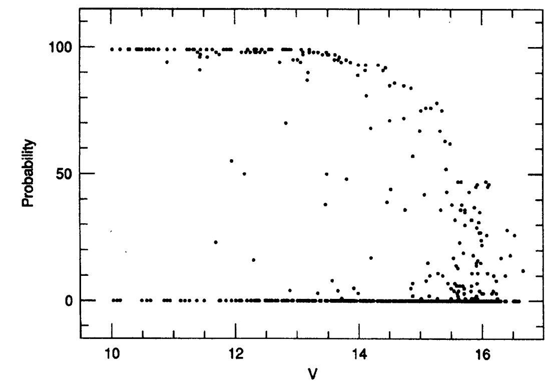

FIG. 5. A plot of membership probabilities vs V magnitude. Note that the membership probabilities for the brighter stars are either 0 or near 100%, while the faint stars have membership probabilities that range between zero and a maximum that decreases with magnitude.

values were obtained for each parameter at half-magnitude steps between V=11.25 and 15.75. Stars within 0.25 mag of these values were assigned the values at these steps and stars brighter than 11.0 where assigned the value of the parameter obtained at 11.25 and those fainter than 16.00 were assigned the value of the parameter obtained at 15.75. The membership probability P is then given by

$$P=100\times\frac{\Phi_c(m,\mu_x,\mu_y,r)}{\Phi(m,\mu_x,\mu_y,r)}.$$

The maximum membership probability possible is a function of magnitude, because both the errors and the ratio of field to cluster stars increase to fainter magnitudes. This is illustrated in Fig. 5, which shows the membership probability plotted against V magnitude. Note that for the brighter stars the membership probabilities essentially give a yes or no answer to cluster membership, while for the faintest stars the maximum membership probability is less than 50%. The membership probability is not an attribute of the star. Obviously, a star is either a member of the cluster or not. Investigators using different data sets or even the same data set and different methodologies will obtain different membership probabilities.

Jones *et al.* (1995) have obtained high dispersion spectra for a large sample of the cluster members, using the HIRES spectrograph on the 10 m Keck telescope and the Hamilton spectrograph on the 3 m Shane telescope. Table 3 gives the preliminary heliocentric radial velocities in km s^{-1} from

TABLE 2. Probability solution parameters.

V	11.19	11.65	12.16	13.12	13.62	14.15	14.67	15.16	15.48	15.68
$\mu_{x,f}$	0.16±0.08	0.16±0.08	0.11±0.07	0.01±0.05	-0.06±0.04	-0.02±0.03	0.04±0.03	0.06±0.03	0.09±0.03	0.11±0.03
$\mu_{y,f}$	0.50 0.09	0.38 0.07	0.28 0.05	0.26 0.04	0.27 0.03	0.28 0.03	0.30 0.02	0.29 0.02	0.31 0.02	0.34 0.02
$\mu_{x,c}$	0.01 0.01	0.01 0.01	0.00 0.01	0.01 0.01	0.02 0.01	0.03 0.01	0.01 0.01	0.02 0.02	0.02 0.03	0.04 0.05
$\mu_{y,c}$	0.01 0.01	0.01 0.01	0.00 0.01	0.01 0.01	0.00 0.01	0.00 0.01	-0.01 0.01	0.02 0.01	0.01 0.03	0.01 0.04
Σ_x	0.29 0.06	0.41 0.06	0.51 0.05	0.47 0.04	0.45 0.03	0.45 0.02	0.46 0.01	0.46 0.02	0.47 0.02	0.48 0.02
Σ_y	0.31 0.06	0.36 0.05	0.38 0.03	0.36 0.03	0.37 0.02	0.38 0.02	0.36 0.02	0.37 0.01	0.38 0.01	0.37 0.02
σ_x	0.06 0.01	0.06 0.01	0.04 0.01	0.04 0.01	0.04 0.01	0.04 0.01	0.07 0.01	0.06 0.02	0.09 0.02	0.17 0.04
σ_y	0.05 0.01	0.05 0.01	0.04 0.01	0.04 0.01	0.05 0.01	0.05 0.01	0.06 0.01	0.04 0.01	0.10 0.04	0.17 0.03
r_o	9.1 3.3	7.7 1.8	5.9 1.0	5.6 0.9	6.2 1.2	6.2 1.6	7.1 2.0	5.3 1.4	5.0 1.5	5.3 1.4

TABLE 3. Radial velocities.

ID	P	v_r km/s	ID	P	v_r km/s
42	76	-8.7	305	98	-6.3
51	99	3.1	317	97	SB2
59	98	-8.4	319	98	-9.3
133	96	-9.6	320	98	VAR?
148	5	VAR	327	0	-7.9
155	95	-7.5	329	98	1.5
156	99	-8.8	331	95	-9.0
158	86	-10.0	335	97	-3.5
167	44	-8.3	356	18	-6.1
168	7	-8.3	362	98	SB2
172	3	-5.0	366	94	-9.8
177	93	-7.7	374	99	-0.4
179	95	-8.7	375	95	-9.5
188	0	-90.3	377	81	-5.6
190	99	-9.0	397	85	-9.5
194	6	-2.2	415	93	-7.6
199	85	-7.0	424	46	-2.8
206	99	-6.8	425	75	-7.8
208	98	-5.2	433	98	-8.0
213	94	-8.1	451	98	-4.3
224	91	-7.4	482	75	-7.7
229	46	-5.5	484	98	-11.5
227	92	-8.8	488	99	-7.0
257	99	-9.0	489	67	-7.0
265	53	-4.5	503	99	-7.6
268	0	-7.8	504	97	-7.7
270	99	VAR?	516	27	-6.4
275	99	-6.9	532	97	-25.7
282	99	SB2	536	47	-2.8
288	57	-13.2	546	99	-7.3
289	76	-8.2	548	99	-6.9
296	91	-67.8	570	72	-7.5
297	99	-8.7	594	94	-8.7
298	71	-5.7	618	8	-9.6
303	95	-7.0			

Jones *et al.* and the membership probabilities obtained here. The errors in radial velocity are typically 3 km s^{-1}. For the most part, the radial velocities tend to confirm the membership probabilities obtained here. We note that most stars have only one observation, so that a discordant radial velocity does not necessarily mean the star is a non-member, since it might be a binary.

Table 4 lists the most discrepant membership probability estimates between those obtained here (JP) and by IS (UV). Listed are stars for which one study gave a probability over 90% and the other less than 50%. In Table 4, columns 1 and 2 give the identification number assigned by us and by IS respectively, columns 4 and 5 the V magnitude and $B-V$ color, columns 5 and 6 the membership probability determined here and by IS. Column 7 gives an estimate as to whether the stars placement in the color–magnitude diagram indicates membership (first letter, Y for membership, N for nonmembership) and whether the radial velocity indicates membership (second letter, Y for membership, N for nonmembership). These stars for the most part have large the errors in one of the studies. A large errors has the effect of giving a star that is a member a low membership probability.

TABLE 4. Discrepant probabilities.

JP	UV	V	B-V	JP%	UV%	mem
59	78	11.70	0.44	98	27	YY
150	116	12.21	0.60	93	34	YY
177	120	14.00	0.79	93	2	YY
190	124	13.08	0.65	99	29	YY
208	133	13.21	0.74	98	49	YY
294	171	10.09		0	90	- -
296	173	14.11	0.75	91	29	YN
317	182	13.42	0.74	97	37	Y -
320	184	13.48	0.80	98	35	Y -
331	188	13.02	0.64	95	47	YY
375	205	13.80	0.79	95	47	YY
434	222	13.62	0.51	97	45	N -
451	231	12.33	0.50	98	40	YY
515	252	13.03	0.63	98	38	Y -
532	257	13.50	0.76	97	25	YN

For example, star JP 294=UV 171 had a large proper motion error in our determination, resulting in a zero membership probability as determined by us. The star is almost certainly a member. This should serve as a caution, in that a zero membership probability does not necessarily mean a star is a nonmember if the associated error for the star is larger than the typical error for a star of that magnitude.

2.5 *Final Results*

Table 5 presents the results for the positions, proper motions, photometry, and membership probabilities determined here. The stars in Table 5 are listed in order of increasing right ascension. Column 1 is a running identification number, columns 2 through 5 give the equatorial coordinates, equator and equinox 1950, columns 6 through 9 are the proper motions and mean errors in x and y (nearly right ascension and declination) in units of arcseconds per century, columns 10 through 12 are the photometry derived here, from CCD observations if colors are given or from photometry of the astrometric plates if not, and column 12 is the membership probability. Table 6 gives cross identifications to other studies. In Table 6, column 1 (JP) is the number assigned here, column 2 (UV) is the number assigned by IS, column 3 (Lv) the number assigned by Latypov (1973) and column 4 (Br) the number assigned by Brüggemann (1937).

The brightest stars in the cluster were too bright for measurement by us, but have proper motion membership determinations by IS. In order to bring together in one place a more complete list of members, we give in Table 7 the stars not measured by us but measured by IS, and for which IS give membership probabilities greater than 40%. We have determined equatorial coordinates for these stars from the (x,y) positions given by IS. For a reference frame, we used our equatorial coordinates for the 190 stars in common. For these reductions, we used our proper motions to produce standard coordinates at the 1927 epoch of the IS positions. We note that our proper motions are relative to (nearly) the cluster motion, and thus the positions we produce at epoch 1927 will be offset in both right ascension and declination. However, for clusters members, the positions we produce

TABLE 5. Positions and proper motions.*

Id	2^h+ min	sec	42°+ ′	″	μ_x	μ_y	σ_x	σ_y	V	B−V	V−I	P
1	37	22.86	29	40.5	0.85	1.77	0.04	0.09	14.38			0
2	37	22.94	29	17.8	0.12	0.49	0.21	0.08	15.79	0.53	0.38	0
3	37	23.68	35	9.5	-0.39	0.20	0.26	0.22	15.62			1
4	37	25.23	28	41.7	4.16	1.12	0.02	0.02	13.79			0
5	37	26.78	34	20.0	0.12	0.61	0.19	0.12	14.94			0
6	37	26.94	26	39.1	0.43	0.14	0.02	0.02	13.16			0
7	37	27.92	31	57.7	0.66	0.75	0.26	0.20	15.76			0
8	37	29.51	36	36.3	-0.77	0.84	0.09	0.07	14.60			0
9	37	30.25	36	24.5	-0.63	-0.17	0.32	0.11	16.06			0
10	37	30.70	27	6.4	-0.25	0.12	0.05	0.04	13.87	0.57	0.49	0
11	37	32.73	27	14.9	-0.30	0.22	0.05	0.05	14.09	0.51	0.43	0
12	37	32.99	29	38.3	-0.27	0.05	0.23	0.35	15.61	0.66	0.62	13
13	37	34.10	38	37.3	2.50	-2.60	0.05	0.06	14.70			0
14	37	34.76	34	52.3	-0.05	0.81	0.20	0.18	15.16	1.00	0.93	0
15	37	36.01	34	58.6	0.56	0.58	0.13	0.24	15.81	0.85	0.75	0
16	37	36.24	38	21.5	-0.89	0.30	0.04	0.05	14.02			0
17	37	36.30	30	5.7	-0.07	-0.01	0.05	0.04	11.55	0.51	0.56	99
18	37	36.42	34	6.2	-0.10	-0.17	0.38	0.10	15.66	1.10	1.09	36
19	37	38.08	36	31.3	-0.30	0.45	0.19	0.12	15.52			0
20	37	38.64	29	16.9	-0.73	1.21	0.06	0.04	14.12			0
21	37	38.97	41	48.4	-0.28	0.51	0.03	0.03	12.79			0
22	37	39.17	28	49.1	-0.02	-0.02	0.03	0.02	12.35			99
23	37	40.33	26	28.7	-0.53	-0.16	0.25	0.24	15.56			0
24	37	40.84	32	29.2	-0.10	0.34	0.07	0.05	14.83			0
25	37	42.87	33	30.9	-0.44	0.38	0.19	0.16	14.97			0
26	37	43.08	42	19.4	-0.64	0.70	0.16	0.21	15.14			0
27	37	43.73	34	58.8	0.45	0.48	0.03	0.02	12.58			0
28	37	44.17	33	37.6	-0.04	0.50	0.05	0.03	14.10			0
29	37	44.17	27	33.2	0.55	1.02	0.08	0.05	14.98			0
30	37	44.26	33	46.2	-0.28	0.32	0.16	0.16	15.19			0
31	37	44.69	33	57.3	0.85	-0.39	0.02	0.02	12.50			0
32	37	44.81	34	11.6	-0.36	0.26	0.33	0.25	15.84			1
33	37	44.94	26	8.7	-0.14	0.29	0.04	0.03	14.34			0
34	37	45.15	30	3.0	0.42	-0.13	0.37	0.14	15.30			0
35	37	45.89	36	28.5	1.33	-1.52	0.04	0.03	11.38			0
36	37	46.88	24	49.3	-0.42	0.10	0.20	0.19	15.86	0.45	0.48	1
37	37	46.90	32	1.0	-0.01	0.59	0.31	0.19	15.61	0.43	0.56	0
38	37	47.19	36	54.6	0.47	0.62	0.31	0.25	16.21	0.77	0.43	0
39	37	47.26	21	2.3	-0.67	-0.16	0.03	0.04	13.86			0
40	37	47.52	35	39.5	0.08	-0.22	0.25	0.14	15.97	0.66	0.61	35
41	37	47.58	39	58.2	-0.29	0.27	0.18	0.12	15.02	0.77	0.93	0
42	37	48.72	29	43.3	0.05	-0.02	0.14	0.16	15.10	1.02	0.88	76
43	37	50.13	45	16.1	-0.59	0.22	0.24	0.16	15.62			0
44	37	50.30	25	3.1	-0.31	-0.07	0.04	0.08	14.96	0.71	0.54	0
45	37	50.32	30	13.5	0.28	0.34	0.19	0.15	15.39	0.79	0.63	0
46	37	51.21	39	3.8	-0.47	0.70	0.08	0.09	15.18	0.58	0.62	0
47	37	51.41	37	43.5	0.02	0.55	0.26	0.11	16.24	0.21	0.37	0
48	37	51.59	32	23.8	-0.28	0.88	0.19	0.26	15.54	0.42	0.50	0
49	37	51.63	43	55.0	-0.23	0.26	0.12	0.05	14.59			0
50	37	51.69	34	3.4	-0.11	0.08	0.02	0.02	13.66	0.01	0.86	4
51	37	51.83	39	50.2	-0.04	0.00	0.05	0.02	11.94	0.42	0.40	99
52	37	52.92	33	32.9	0.03	0.18	0.42	0.11	16.08	0.34	1.56	26
53	37	53.26	27	11.7	-0.03	0.03	0.04	0.04	10.91	0.25	0.14	99
54	37	53.83	41	10.8	-0.67	0.65	0.14	0.25	15.44			0
55	37	54.07	30	12.6	-0.20	0.61	0.45	0.26	16.51	0.69	0.55	0
56	37	54.51	29	4.1	0.93	0.32	0.03	0.03	12.26			0
57	37	54.73	44	13.8	-0.43	0.37	0.39	0.32	15.87			0
58	37	54.76	36	54.0	-0.26	0.51	0.20	0.16	15.77	0.48	0.62	0
59	37	55.21	38	39.9	-0.08	0.02	0.02	0.05	11.70	0.44	0.33	98
60	37	55.22	35	42.8	0.63	0.96	0.34	0.26	16.56	0.62	0.45	0
61	37	55.36	41	28.9	-0.02	0.00	0.22	0.16	16.07	0.63	0.79	47
62	37	55.94	20	48.5	0.16	0.69	0.08	0.07	14.71	0.52	0.41	0
63	37	55.99	38	29.1	0.18	0.35	0.08	0.10	16.01	0.95	0.77	3
64	37	56.47	31	27.7	-0.45	0.01	0.28	0.61	16.25	0.44	0.54	1
65	37	56.64	33	5.4	0.02	0.02	0.02	0.02	12.88	-0.11	0.75	99
66	37	57.11	24	6.9	0.04	0.39	0.08	0.08	14.45	0.62	0.55	0
67	37	58.20	32	59.9	2.43	0.52	0.03	0.01	13.28			0
68	37	58.43	43	59.5	0.03	0.47	0.13	0.13	14.97			0
69	37	58.45	27	45.9	0.01	0.03	0.06	0.03	10.43			99
70	37	59.53	37	31.2	-1.36	0.27	0.32	0.27	15.94			0
71	37	59.72	35	45.9	0.22	0.45	0.25	0.20	15.83	0.87	0.86	0
72	37	59.73	40	47.8	0.05	0.43	0.04	0.04	14.43	0.48	0.54	0
73	38	0.16	46	52.6	-1.86	1.10	0.02	0.02	12.31			0
74	38	0.19	18	58.4	-0.15	0.54	0.34	0.16	15.37			0
75	38	0.43	20	8.5	-0.06	0.22	0.18	0.24	15.54	0.66	0.53	17
76	38	0.72	45	58.3	-0.31	0.69	0.02	0.01	11.74			0
77	38	0.77	44	56.7	0.11	0.61	0.17	0.12	15.20			0
78	38	0.85	20	47.7	-0.04	0.24	0.07	0.05	14.87	0.47	0.39	0
79	38	1.43	27	22.9	0.08	-0.10	0.03	0.02	13.49	0.57	0.48	50
80	38	2.39	37	57.7	0.14	0.04	0.33	0.12	15.52	0.55	0.38	38
81	38	3.39	42	20.4	-4.27	-1.61	0.03	0.03	13.08			0
82	38	3.47	22	21.7	-0.70	0.38	0.22	0.15	15.84			0
83	38	3.68	26	34.5	-0.54	0.30	0.24	0.20	15.99	0.34	0.51	0
84	38	3.84	46	5.4	0.19	0.29	0.03	0.05	10.90			0
85	38	3.87	37	58.3	-0.32	-0.37	0.17	0.09	15.08	0.80	0.71	0
86	38	4.32	29	24.6	0.14	0.33	0.67	0.21	16.18	0.61	0.51	4
87	38	4.33	30	44.1	0.01	0.05	0.04	0.05	10.46	0.18	0.00	99
88	38	4.39	31	27.9	0.03	0.33	0.07	0.05	14.60	1.07	1.09	0
89	38	4.68	21	28.6	0.47	-0.05	0.03	0.02	13.57			0
90	38	5.41	47	28.6	4.25	-3.06	0.38	0.22	15.94			0
91	38	5.58	19	41.4	-0.19	0.37	0.46	0.40	15.30	0.49	0.51	0
92	38	5.69	42	43.3	0.35	0.55	0.27	0.29	15.80	0.81	0.63	0
93	38	6.20	39	13.5	-0.67	0.35	0.04	0.04	14.13			0
94	38	6.31	46	3.8	-0.32	0.47	0.21	0.20	15.50	0.83	0.58	0
95	38	6.40	28	22.0	-0.27	0.95	0.14	0.15	15.93	0.54	0.40	0
96	38	6.82	28	9.2	-0.70	0.13	0.44	0.28	16.56	0.56	0.62	0
97	38	6.96	47	9.3	-0.10	0.13	0.03	0.03	12.30	0.50	0.43	16
98	38	7.09	33	18.0	-0.56	0.29	0.06	0.06	14.98			0
99	38	7.36	36	19.4	0.76	0.54	0.02	0.03	11.76			0
100	38	7.44	39	52.9	-0.03	0.00	0.03	0.05	10.30	0.16	-0.02	99
101	38	7.75	18	35.9	-1.13	0.30	0.03	0.02	13.03			0
102	38	7.89	25	5.9	0.34	0.12	0.16	0.15	15.48	0.49	0.49	0
103	38	7.89	46	31.5	-0.76	-0.21	0.02	0.02	13.12			0
104	38	8.02	38	21.1	-0.34	0.90	0.53	0.35	16.04	0.51	0.48	0
105	38	8.33	22	56.8	0.21	0.03	0.10	0.09	15.16	0.98	0.89	10
106	38	8.78	34	50.9	0.71	-0.11	0.18	0.09	14.77			0
107	38	8.80	18	14.1	0.61	1.45	0.30	0.24	15.55			0
108	38	9.07	19	48.0	-0.98	0.54	0.16	0.16	15.25			0
109	38	9.33	45	33.7	-1.04	0.31	0.21	0.15	14.89			0
110	38	9.55	19	54.3	0.41	0.34	0.04	0.02	12.19			0
111	38	9.71	28	22.4	0.13	0.11	0.16	0.20	15.83	0.51	0.63	32
112	38	9.74	43	37.7	0.14	0.69	0.03	0.02	13.70			0
113	38	9.92	27	28.6	-0.02	-0.05	0.24	0.10	14.86	0.88	0.91	84
114	38	10.02	45	48.7	0.14	-0.07	0.02	0.03	12.16	0.66	0.60	50
115	38	10.66	36	15.6	-0.03	-0.07	0.04	0.09	10.15	0.18	-0.06	99
116	38	10.77	18	8.3	0.16	0.60	0.06	0.05	14.87	0.97	0.99	0
117	38	10.84	35	31.2	-0.14	0.18	0.08	0.07	14.59	1.41	0.71	0
118	38	10.85	41	29.6	0.07	-0.02	0.08	0.04	14.32	0.54	0.51	93
119	38	10.88	42	35.3	-0.36	0.34	0.62	0.37	16.07	0.58	0.61	0
120	38	11.21	35	37.3	0.61	0.92	0.12	0.07	14.87			0
121	38	11.80	42	35.8	-0.47	0.59	0.04	0.06	14.31			0
122	38	12.24	37	46.0	0.48	-0.16	0.04	0.05	10.14			0
123	38	12.61	29	53.9	-0.08	0.62	0.05	0.05	14.31	0.93	0.86	0
124	38	12.91	35	25.7	-0.01	0.02	0.01	0.01	13.35	0.64	0.58	98
125	38	13.08	22	16.9	0.31	-0.14	0.17	0.22	15.58	0.52	0.58	14
126	38	13.09	33	34.7	0.04	0.54	0.05	0.03	14.22	1.14	1.07	0
127	38	13.60	25	20.5	0.80	0.57	0.17	0.27	15.68			0
128	38	13.81	35	25.5	0.59	0.49	0.20	0.20	15.27			0
129	38	13.93	30	54.9	-0.65	0.29	0.17	0.14	15.15			0
130	38	14.20	21	8.7	-0.06	0.46	0.25	0.15	15.40	0.90	0.93	0
131	38	14.57	22	54.9	-0.66	0.01	0.31	0.11	14.77			0
132	38	14.88	46	8.2	-0.47	0.82	0.22	0.18	15.84			0
133	38	14.98	25	49.9	0.06	0.03	0.03	0.03	13.69	0.66	0.68	96
134	38	15.47	18	38.3	0.13	0.82	0.14	0.13	14.88	0.98	0.84	0
135	38	15.61	24	23.2	-0.05	0.67	0.21	0.30	15.61	0.55	0.46	0
136	38	15.66	27	2.4	-0.26	0.14	0.06	0.07	14.66	0.57	0.50	0
137	38	15.68	20	50.5	0.00	0.07	0.04	0.03	10.62	0.33	0.25	99
138	38	15.75	40	6.7	-0.38	0.71	0.28	0.09	14.90			0
139	38	15.95	24	15.1	-0.12	0.30	0.33	0.13	15.59	0.83	0.77	6
140	38	16.03	32	24.4	-0.37	0.65	0.03	0.02	13.12			0
141	38	16.96	30	22.8	-0.59	0.37	0.04	0.03	14.11			0
142	38	18.15	36	33.7	-0.01	0.72	0.23	0.57	16.13	0.58	0.48	0
143	38	18.39	40	24.6	-0.28	0.30	0.03	0.04	14.20	0.56	0.50	0
144	38	18.68	20	44.3	-0.06	0.95	0.29	0.13	16.06	0.74	0.64	0
145	38	18.96	41	54.9	-0.13	0.06	0.38	0.14	15.84	0.97	0.87	32
146	38	19.65	23	55.0	0.05	-0.01	0.02	0.02	12.32	0.56	0.48	99
147	38	20.08	46	3.0	1.05	-0.53	0.16	0.16	15.34			0
148	38	20.18	29	24.9	-0.12	-0.03	0.03	0.02	13.92	0.75	0.68	5
149	38	20.36	29	59.7	0.03	0.71	0.02	0.01	12.33			0
150	38	20.56	19	35.3	-0.04	0.01	0.02	0.02	12.21	0.60	0.53	99
151	38	20.89	39	42.8	0.36	0.19	0.07	0.04	14.72	0.71	0.71	0
152	38	20.95	30	18.9	-0.68	-0.10	0.38	0.31	16.25	0.91	0.88	0
153	38	20.97	29	13.4	1.20	-0.94	0.02	0.02	13.08			0
154	38	21.25	39	17.3	0.36	-0.18	0.40	0.15	15.92	1.31	1.18	7
155	38	21.28	33	5.1	0.08	0.01	0.02	0.01	12.95	0.59	0.52	95
156	38	21.58	44	19.1	-0.01	-0.02	0.01	0.02	11.82	0.56	0.46	99
157	38	21.76	44	52.8	-0.13	-0.18	0.29	0.14	15.95	1.39	1.15	31
158	38	22.01	28	15.6	0.03	0.04	0.09	0.03	14.59	0.84	0.89	86
159	38	22.02	20	44.0	-0.14	-0.22	0.04	0.04	14.07	0.91	0.86	0
160	38	22.10	30	14.3	0.15	0.54	0.12	0.06	14.81	0.52	0.43	0
161	38	22.25	18	16.5	-0.14	0.57	0.19	0.22	14.99	0.54	0.51	0
162	38	22.58	24	25.5	0.44	0.70	0.05	0.04	14.38			0
163	38	22.68	25	33.6	1.68	-0.10	0.12	0.17	15.13			0
164	38	22.73	43	58.0	-0.04	0.91	0.05	0.04	14.21	0.59	0.52	0
165	38	22.97	21	47.5	0.01	0.01	0.02	0.02	12.83	0.62	0.62	99
166	38	23.11	18	16.0	-0.78	0.13	0.02	0.02	12.52			0
167	38	23.16	37	33.3	-0.09	-0.12	0.07	0.09	14.53	0.87	0.80	44
168	38	23.19	32	19.6	-0.33	-0.02	0.28	0.31	15.92	0.85	0.77	7
169	38	23.38	34	31.0	-0.24	0.40	0.06	0.05	14.51	0.67	0.56	0
170	38	23.51	29	6.4	-0.30	0.75	0.07	0.09	15.12	0.92	0.87	0
171	38	23.77	46	52.9	-0.03	0.17	0.04	0.03	13.99	0.79	0.40	3
172	38	23.93	44	35.0	-0.06	0.37	0.28	0.12	15.71	1.15	1.12	3
173	38	24.11	21	28.3	1.65	-0.41	0.17	0.23	16.08			0
174	38	24.63	42	56.2	0.21	1.02	0.25	0.29	16.03			0
175	38	24.67	32	0.2	-0.28	0.24	0.25	0.15	16.00	0.68	0.64	3
176	38	24.80	41	9.3	-0.11	0.57	0.32	0.09	15.83			0
177	38	24.82	31	17.7	0.04	-0.07	0.03	0.04	14.00	0.79	0.74	93
178	38	25.24	35	50.4	-0.01	0.92	0.07	0.08	14.84	0.67	0.63	0
179	38	25.26	26	17.7	-0.01	0.05	0.01	0.02	13.61	0.68	0.72	95
180	38	25.46	26	24.5	-0.12	0.25	0.08	0.06	14.65	0.51	0.06	0
181	38	25.70	31	27.6	-1.23	0.29	0.33	0.24	16.30			0
182	38	25.82	47	28.1	2.42	-1.03	0.27	0.43	15.06			0
183	38	25.90	47	34.2	-0.18	0.50	0.04	0.05	10.63			0
184	38	26.18	39	58.5	-0.04	-0.03	0.04	0.05	10.43	0.24	0.01	99
185	38	26.71	24	35.1	0.58	0.67	0.10	0.06	15.11			0
186	38	26.73	29	33.7	-0.08	0.41	0.03	0.03	11.26	1.00	1.03	0
187	38	26.86	43	40.7	0.04	0.01	0.29	0.15	15.62	0.69	0.63	47
188	38	26.91	25	0.3	0.07	0.40	0.05	0.07	14.60	0.88	0.94	0
189	38	26.99	38	24.7	0.18	0.50	0.13	0.10	15.15	0.59	0.56	0
190	38	27.23	42	0.5	0.03	-0.01	0.01	0.01	13.08	0.65	0.59	99
191	38	28.01	33	31.4	0.00	-0.05	0.03	0.05	10.50	0.12	0.09	99
192	38	28.18	41	17.0	0.71	0.64	0.19	0.16	15.37			0
193	38	28.23	48	14.5	-0.16	0.08	0.27	0.10	15.10	0.72	0.71	8
194	38	28.27	45	10.6	-0.35	-0.08	0.29	0.15	15.64	1.27	1.09	6
195	38	28.68	22	57.3	0.96	0.41	0.07	0.05	15.01			0
196	38	29.38	22	59.9	-0.07	0.34	0.19	0.21	15.48	0.98	0.93	0
197	38	29.83	20	27.1	0.38	-0.18	0.29	0.14	15.71	0.98	1.23	5
198	38	30.63	27	45.7	3.02	-1.40	0.32	0.30	15.64			0
199	38	30.79	33	21.2	0.07	0.02	0.04	0.03	14.51	0.91	0.80	85
200	38	30.80	23	22.3	-0.07	-0.10	0.02	0.04	13.47	0.73	0.72	38

*Table 5 can also be found in the AAS CD-ROM, Volume X, 1996.

TABLE 5. (continued)

Id	2^h+ min	sec	$42^\circ+$ ′	″	μ_x	μ_y	σ_x	σ_y	V	B−V	V−I	P
201	38	30.90	27	8.7	-0.42	-0.08	0.03	0.03	13.87			0
202	38	31.02	35	26.9	-0.02	0.88	0.30	0.33	16.10	0.47	0.57	0
203	38	31.27	20	6.3	-0.10	1.03	0.20	0.35	16.04	0.62	0.46	0
204	38	31.60	49	25.2	0.07	0.75	0.25	0.25	14.94			0
205	38	31.87	29	30.0	0.04	0.13	0.04	0.02	13.81	1.13	1.06	48
206	38	32.07	36	14.1	0.02	-0.02	0.01	0.01	12.55	0.52	0.49	99
207	38	32.26	43	29.5	-0.37	0.50	0.09	0.14	15.18	0.83	0.72	0
208	38	32.63	30	3.8	-0.02	-0.01	0.03	0.01	13.21	0.74	0.69	98
209	38	33.60	16	44.4	-0.47	-0.58	0.04	0.03	12.49			0
210	38	33.66	46	46.9	-0.05	0.71	0.03	0.03	13.38			0
211	38	33.76	30	10.2	0.03	0.05	0.03	0.02	11.27	0.29	0.25	99
212	38	33.93	37	22.6	-0.01	0.33	0.03	0.03	13.75			0
213	38	34.06	30	52.5	0.07	-0.05	0.03	0.02	13.07	0.60	0.57	94
214	38	34.14	45	2.2	-0.15	0.23	0.19	0.27	15.93	0.67	0.84	11
215	38	34.63	28	32.3	-0.72	0.10	0.02	0.01	12.25	0.59	0.60	0
216	38	34.80	26	17.6	-0.02	0.00	0.02	0.02	12.88	0.57	0.51	99
217	38	34.91	33	16.0	0.46	0.43	0.15	0.09	15.08			0
218	38	34.99	36	47.4	0.26	-0.21	0.38	0.26	16.31	1.08	1.34	17
219	38	35.05	36	18.8	0.01	-0.08	0.02	0.01	12.73	0.45	0.42	94
220	38	35.30	34	18.0	-0.33	0.76	0.06	0.18	15.61	0.86	0.84	0
221	38	35.59	26	47.2	-0.03	-0.20	0.18	0.16	15.68	0.65	0.72	38
222	38	35.62	49	7.3	0.65	0.98	0.03	0.03	12.92			0
223	38	35.77	18	45.0	-0.85	0.64	0.01	0.02	13.58			0
224	38	36.18	23	51.3	-0.02	0.01	0.05	0.05	14.40	0.84	0.76	91
225	38	36.26	31	41.9	-0.27	-1.17	0.14	0.22	15.84			0
226	38	36.34	32	47.1	-0.10	0.06	0.21	0.30	15.73	0.68	0.58	36
227	38	36.74	24	27.6	0.07	-0.03	0.04	0.04	14.44	0.83	0.79	92
228	38	36.82	44	34.3	-1.35	0.59	0.27	0.30	16.19			0
229	38	36.94	31	51.5	-0.04	0.00	0.29	0.23	16.12	1.37	1.27	46
230	38	37.24	25	44.0	0.01	0.63	0.01	0.01	12.60			0
231	38	37.30	38	51.9	0.07	-0.01	0.02	0.02	11.45	0.33	0.30	99
232	38	37.33	22	11.0	0.71	0.95	0.36	0.42	16.00	0.62	0.67	0
233	38	37.41	49	12.2	-0.55	0.42	0.19	0.14	15.21			0
234	38	37.53	22	47.8	0.16	0.11	0.39	0.21	16.41	0.91	0.93	28
235	38	37.60	41	26.0	-0.30	0.73	0.04	0.04	14.38	1.03	0.90	0
236	38	37.69	17	52.6	-0.03	0.18	0.02	0.02	13.30	0.99	0.86	0
237	38	37.69	47	22.7	0.20	0.06	0.29	0.26	15.92	0.87	0.80	29
238	38	37.91	42	50.5	-0.37	1.12	0.11	0.06	14.89			0
239	38	37.97	32	12.9	-0.43	0.36	0.08	0.04	14.45	0.55	0.53	0
240	38	37.97	41	14.2	0.14	0.20	0.04	0.08	14.51	0.58	0.52	0
241	38	38.17	21	38.6	-0.40	-0.15	0.09	0.06	14.95	0.85	0.93	0
242	38	38.26	32	3.1	-0.23	0.48	0.30	0.17	15.86	0.64	0.59	0
243	38	38.34	31	16.0	1.04	-0.04	0.53	0.31	16.51	1.00	0.94	0
244	38	38.38	33	34.2	-0.09	-0.33	0.06	0.06	14.37	0.88	0.80	0
245	38	38.71	29	20.6	-0.19	0.30	0.15	0.12	15.12	0.55	0.47	0
246	38	38.90	31	51.5	-0.01	0.07	0.02	0.02	12.18	0.48	0.45	98
247	38	38.94	28	2.3	-0.30	0.74	0.05	0.04	14.39	0.52	0.51	0
248	38	39.13	24	41.7	0.47	0.50	0.23	0.10	15.03			0
249	38	39.19	35	1.6	-0.35	0.87	0.01	0.02	13.46			0
250	38	39.32	30	17.3	-0.08	0.46	0.03	0.02	13.37			0
251	38	39.74	40	31.7	-0.10	-0.14	0.02	0.02	13.72	0.74	0.62	1
252	38	40.16	16	49.8	0.16	0.10	0.20	0.25	15.13	0.85	0.80	15
253	38	40.52	46	49.8	-0.17	0.55	0.19	0.29	16.27	1.36	1.31	0
254	38	40.86	39	54.3	-0.21	0.39	0.16	0.17	14.99	1.06	0.99	0
255	38	40.88	24	42.4	0.54	-0.09	0.16	0.12	15.31			0
256	38	41.17	27	37.7	-0.31	0.62	0.03	0.03	11.12	0.97	0.99	0
257	38	41.22	34	58.3	-0.01	0.04	0.01	0.03	12.34	0.46	0.61	99
258	38	41.44	40	7.4	-0.33	0.07	0.06	0.06	14.36	0.83	0.79	0
259	38	41.95	35	6.0	0.83	-0.12	0.16	0.15	15.14			0
260	38	42.14	48	55.7	1.06	-1.68	0.02	0.02	12.36			0
261	38	42.97	19	46.8	0.65	0.65	0.41	0.25	16.19	0.66	0.55	0
262	38	43.16	29	32.9	-0.21	0.30	0.17	0.36	16.02	0.78	0.62	3
263	38	43.61	30	7.3	0.05	0.06	0.17	0.19	15.33	0.63	0.51	67
264	38	43.68	33	2.4	-0.34	0.62	0.52	0.35	16.26	0.68	0.71	0
265	38	43.71	47	40.8	0.04	-0.12	0.36	0.26	15.43	1.15	1.19	53
266	38	44.05	36	2.7	-0.10	0.67	0.35	0.20	14.87	0.85	0.94	0
267	38	44.09	46	3.5	-0.51	-0.03	0.21	0.20	15.03	0.81	0.68	0
268	38	44.32	40	36.7	-0.12	-0.27	0.36	0.27	16.00	1.16	1.35	22
269	38	44.35	32	51.6	1.40	-0.39	0.24	0.26	15.57			0
270	38	44.38	36	2.6	0.02	0.00	0.03	0.02	12.60	0.60	0.48	99
271	38	44.40	49	2.2	-0.61	0.65	0.34	0.36	15.96			0
272	38	44.53	27	16.8	0.77	-0.54	0.12	0.15	15.08			0
273	38	44.84	16	31.5	-0.09	0.33	0.21	0.18	15.50	0.65	0.42	5
274	38	44.93	40	37.3	0.12	-0.34	0.17	0.24	15.98	0.88	0.95	15
275	38	44.97	33	17.4	0.03	0.02	0.02	0.01	11.92	0.44	0.43	99
276	38	45.04	44	44.5	-0.10	0.39	0.22	0.34	15.91			2
277	38	45.09	40	43.3	0.17	0.38	0.03	0.03	13.79			0
278	38	45.13	47	16.9	-0.90	0.12	0.25	0.15	14.97			0
279	38	45.57	26	31.8	0.10	0.08	0.03	0.02	11.44	0.32	0.25	96
280	38	46.24	28	16.2	0.08	-0.06	0.02	0.02	13.18	0.70	0.71	87
281	38	46.81	38	14.4	-0.14	0.36	0.03	0.03	14.48	0.54	0.46	0
282	38	46.92	36	7.8	0.01	0.00	0.01	0.02	12.80	0.75	0.71	99
283	38	47.20	44	58.3	-0.09	0.42	0.14	0.17	15.02			0
284	38	47.42	30	51.1	0.04	0.89	0.43	0.20	16.07	0.50	0.50	0
285	38	47.53	44	51.5	-0.03	0.55	0.03	0.02	13.05			0
286	38	47.94	33	17.9	0.23	1.10	0.32	0.23	15.17			0
287	38	48.13	20	15.7	-0.98	0.66	0.02	0.03	13.81			0
288	38	48.45	48	27.9	-0.05	-0.11	0.19	0.17	14.89	1.06	0.96	57
289	38	48.97	39	6.0	0.03	-0.04	0.18	0.24	15.18	0.95	0.97	76
290	38	49.41	18	12.3	-0.04	-0.07	0.05	0.04	11.40	0.74	0.65	98
291	38	49.45	27	7.6	0.14	0.70	0.03	0.03	14.03	1.25	1.10	0
292	38	49.49	34	14.7	0.29	0.07	0.02	0.03	11.85	0.19	0.19	0
293	38	50.78	49	51.0	-0.36	0.40	0.24	0.20	15.92	0.68	0.71	0
294	38	50.81	20	4.1	-0.05	-0.72	0.53	0.94	10.09			0
295	38	50.95	26	59.9	0.99	-0.45	0.15	0.20	16.15			0
296	38	52.01	28	9.7	0.09	0.01	0.03	0.04	14.11	0.75	0.72	91
297	38	52.08	38	17.2	-0.02	-0.02	0.02	0.01	12.44	0.56	0.46	99
298	38	52.30	34	8.2	0.10	0.04	0.04	0.04	14.51	1.01	1.00	71
299	38	52.72	16	23.7	0.74	0.50	0.04	0.05	14.22			0
300	38	52.90	25	41.4	-0.10	0.54	0.05	0.03	14.30	0.63	0.56	0
301	38	52.96	33	11.4	-0.01	-0.09	0.03	0.03	10.77	0.20	0.18	99
302	38	53.20	29	26.2	0.92	0.29	0.02	0.02	12.56	0.41	0.59	0
303	38	53.35	23	35.5	0.06	0.04	0.02	0.02	13.67	0.85	0.82	95
304	38	53.36	37	53.1	0.90	0.41	0.18	0.33	15.52			0
305	38	53.38	35	1.2	-0.05	-0.02	0.01	0.02	12.41	0.52	0.49	98
306	38	53.41	42	18.1	1.11	0.72	0.08	0.12	15.27			0
307	38	53.48	29	13.0	-0.20	-0.24	0.08	0.04	14.16	0.59	0.62	0
308	38	53.76	30	33.9	0.19	-0.10	0.26	0.19	15.37	0.70	0.72	10
309	38	53.84	37	55.4	1.04	-0.21	0.32	0.26	16.60			0
310	38	54.01	34	41.5	-0.06	-0.21	0.26	0.08	15.73	1.25	1.19	35
311	38	54.19	19	35.6	0.70	0.16	0.06	0.06	14.57			0
312	38	54.19	23	0.3	-0.83	-1.12	0.09	0.07	14.91			0
313	38	54.28	25	20.1	-0.37	-0.02	0.23	0.15	15.96	0.56	0.45	4
314	38	54.46	24	26.5	0.46	0.25	0.24	0.12	15.59			0
315	38	54.90	25	56.7	-0.03	0.03	0.02	0.02	13.11	0.60	0.55	97
316	38	55.09	35	6.6	2.52	-1.24	0.05	0.13	14.69			0
317	38	55.35	29	1.7	-0.01	-0.05	0.03	0.03	13.42	0.74	0.72	97
318	38	55.74	35	22.1	-0.16	0.75	0.07	0.06	14.67	0.89	0.92	0
319	38	55.85	36	57.5	0.04	-0.01	0.02	0.01	13.11	0.79	0.57	98
320	38	56.01	29	20.3	0.02	-0.03	0.01	0.02	13.48	0.80	0.80	98
321	38	56.01	28	25.1	-0.28	0.17	0.26	0.33	15.83	0.57	0.56	6
322	38	56.37	34	54.2	-0.34	0.17	0.29	0.26	16.23	0.87	0.73	3
323	38	56.66	32	26.1	0.06	-0.02	0.02	0.03	11.23	0.26	0.22	99
324	38	56.76	21	12.7	-0.18	0.36	0.29	0.14	15.30	0.62	0.64	0
325	38	56.99	37	52.1	-0.22	0.31	0.03	0.02	13.66			0
326	38	57.04	37	11.3	-0.09	-1.14	0.04	0.16	10.03			0
327	38	57.74	37	51.3	-0.14	-0.09	0.06	0.03	14.49	0.91	0.91	0
328	38	57.85	36	39.8	0.29	0.11	0.45	0.23	16.67	0.77	0.63	12
329	38	57.86	17	51.7	-0.03	-0.05	0.03	0.02	12.11	0.48	0.39	98
330	38	58.29	31	3.1	-0.18	-0.20	0.07	0.15	15.64	1.05	1.13	23
331	38	58.40	46	14.1	0.06	0.05	0.02	0.02	13.02	0.64	0.59	95
332	38	58.64	34	25.8	-0.02	-0.06	0.05	0.08	10.02	0.08	-0.03	99
333	38	58.73	22	54.3	-0.22	0.78	0.14	0.21	15.28	0.69	0.68	0
334	38	59.23	30	34.2	0.57	-0.21	0.11	0.15	14.74			0
335	38	59.53	30	54.0	0.03	0.04	0.02	0.01	13.52	0.69	0.62	97
336	38	59.59	42	59.1	1.51	0.23	0.02	0.01	12.83			0
337	38	59.62	37	19.6	-0.04	0.28	0.24	0.33	16.38	0.77	0.49	10
338	38	59.74	24	31.8	0.05	-0.01	0.03	0.03	11.03	0.38	0.31	99
339	38	59.80	35	43.4	0.24	1.02	0.22	0.11	16.21	0.84	0.66	0
340	39	0.04	27	14.5	-0.42	0.78	0.14	0.22	15.94			0
341	39	0.10	28	12.6	0.17	0.37	0.26	0.17	15.61	0.72	0.64	2
342	39	0.26	43	3.0	0.05	0.16	0.02	0.03	14.20	0.92	0.95	17
343	39	0.52	38	38.5	0.90	-3.87	0.01	0.01	12.19			0
344	39	0.54	47	13.8	-0.60	0.36	0.31	0.25	16.05	0.65	0.78	0
345	39	0.90	40	4.9	1.70	-0.29	0.03	0.05	10.49			0
346	39	1.22	41	48.5	0.27	-0.04	0.02	0.02	13.18	0.69	0.64	0
347	39	1.75	18	40.5	-1.08	0.97	0.24	0.21	15.69			0
348	39	1.77	21	16.3	-0.17	0.55	0.18	0.42	16.25	0.46	0.51	0
349	39	1.81	15	50.9	0.28	0.27	0.06	0.10	13.62			0
350	39	1.87	35	48.0	-0.17	0.59	0.18	0.22	15.14	1.05	0.99	0
351	39	2.47	36	6.6	0.50	0.23	0.13	0.20	16.12	0.92	0.77	0
352	39	2.83	40	3.2	-0.08	0.10	0.03	0.02	11.44	0.34	0.29	91
353	39	3.14	38	47.1	0.29	0.70	0.23	0.25	15.93	0.76	0.75	0
354	39	3.55	31	50.8	0.24	0.66	0.10	0.14	15.46	1.10	1.09	0
355	39	3.56	23	22.5	-1.61	0.24	0.01	0.02	12.10			0
356	39	3.69	35	33.8	0.29	-0.09	0.23	0.29	15.86	1.16	1.26	18
357	39	4.17	36	18.5	-2.21	0.80	0.28	0.16	15.63			0
358	39	4.18	22	19.0	0.09	0.27	0.39	0.31	15.84	0.32	0.35	11
359	39	4.73	31	7.2	-0.01	0.19	0.10	0.20	15.45	0.50	0.51	7
360	39	4.74	30	36.3	0.14	0.77	0.16	0.19	15.74	0.64	0.56	0
361	39	5.31	32	24.6	-1.47	0.07	0.03	0.05	14.46			0
362	39	5.41	34	4.0	-0.05	0.00	0.01	0.02	12.49	0.61	0.56	98
363	39	5.80	21	42.3	18.56	4.31	0.21	0.17	16.37			0
364	39	5.93	22	30.0	-0.71	0.89	0.33	0.25	15.80			0
365	39	5.98	37	31.1	0.42	-0.04	0.19	0.24	15.62	0.86	0.78	4
366	39	6.10	17	19.4	0.03	-0.08	0.04	0.06	13.72	0.73	0.65	94
367	39	6.38	37	48.7	-0.10	0.32	0.24	0.27	15.71	0.71	0.58	5
368	39	6.59	29	51.7	0.49	0.91	0.40	0.15	15.58			0
369	39	6.92	42	51.6	0.15	0.40	0.16	0.14	15.11	0.67	0.67	0
370	39	7.36	33	57.4	0.67	1.02	0.12	0.21	15.51			0
371	39	7.39	30	53.6	0.53	-0.05	0.16	0.08	15.23	1.02	0.97	0
372	39	7.75	34	51.9	0.24	0.81	0.17	0.12	15.95	0.55	0.46	0
373	39	8.04	19	12.5	0.21	0.16	0.03	0.03	13.76	0.53	0.43	0
374	39	8.29	18	43.3	-0.01	-0.02	0.01	0.03	11.64	0.44	0.37	99
375	39	8.51	46	28.7	-0.03	0.00	0.06	0.04	13.80	0.79	0.77	95
376	39	8.56	32	59.0	0.09	0.44	0.04	0.05	13.59			0
377	39	8.71	19	28.2	0.08	-0.09	0.04	0.04	14.13	0.94	0.90	81
378	39	9.05	21	45.4	0.13	-0.08	0.06	0.07	15.08	0.51	0.52	42
379	39	9.15	37	5.9	1.30	0.19	0.05	0.05	14.85			0
380	39	9.18	44	44.4	0.27	0.01	0.09	0.05	14.58	0.85	0.80	0
381	39	9.24	41	38.0	-0.40	0.63	0.27	0.11	16.29	0.69	0.74	0
382	39	9.43	23	17.6	0.06	1.04	0.06	0.04	11.19			0
383	39	9.56	17	32.8	0.02	0.24	0.03	0.04	13.95	1.08	0.99	0
384	39	10.39	19	46.7	4.75	-5.05	0.03	0.02	13.39			0
385	39	10.77	36	49.5	4.80	-0.73	0.02	0.03	12.01			0
386	39	11.21	22	51.1	0.18	0.83	0.21	0.26	15.64	0.61	0.69	0
387	39	11.27	18	13.8	0.19	-0.11	0.02	0.03	13.06	0.89	0.84	0
388	39	11.86	42	7.4	-0.23	0.80	0.52	0.41	16.05	0.60	0.79	0
389	39	12.05	44	18.2	-0.14	0.83	0.28	0.17	15.69	0.56	0.56	0
390	39	12.10	19	36.8	0.43	-0.05	0.08	0.05	15.13	0.80	0.77	0
391	39	12.15	36	21.1	0.66	0.40	0.27	0.15	15.25			0
392	39	12.21	28	24.3	-0.05	0.05	0.26	0.15	15.49	1.01	1.02	62
393	39	12.62	44	57.2	-0.41	-0.68	0.27	0.13	15.52			0
394	39	12.71	38	33.0	-0.23	0.46	0.02	0.03	13.96	0.55	0.49	0
395	39	12.71	15	59.8	0.72	-0.32	0.05	0.10	14.11			0
396	39	12.83	30	57.2	-0.05	0.30	0.08	0.11	14.81			0
397	39	13.17	17	28.8	-0.04	-0.04	0.17	0.13	14.74	0.90	0.83	85
398	39	13.61	49	17.9	0.27	-0.16	0.23	0.18	14.83	0.78	0.64	0
399	39	13.62	45	-22.0	0.82	0.28	0.17	0.11	14.97			0
400	39	13.67	37	4.9	-0.12	-0.12	0.02	0.02	12.89	0.59	0.57	4

TABLE 5. (continued)

	2^h+		42°+									
Id	min	sec	′	″	μ_x	μ_y	σ_x	σ_y	V	B−V	V−I	P
401	39	13.80	33	40.6	0.61	0.35	0.08	0.13	15.12			0
402	39	13.82	43	37.8	-0.38	0.84	0.14	0.12	14.98			0
403	39	13.88	43	22.5	0.21	0.43	0.25	0.16	15.92	0.89	0.80	1
404	39	14.21	33	31.8	0.02	-0.02	0.02	0.02	12.34	0.52	0.49	99
405	39	14.28	23	37.0	0.04	0.28	0.40	0.16	16.09	0.72	0.83	11
406	39	14.67	33	1.5	0.05	0.24	0.25	0.19	15.93	0.62	0.48	16
407	39	14.80	32	17.1	0.18	-0.21	0.30	0.19	15.96	1.19	1.20	27
408	39	15.80	49	32.8	0.35	0.27	0.04	0.03	13.02			0
409	39	16.23	29	12.3	1.24	0.26	0.07	0.05	14.70			0
410	39	16.28	23	21.6	0.46	0.47	0.03	0.03	10.95			0
411	39	16.39	25	12.5	-0.09	0.74	0.19	0.12	15.01	0.48	0.50	0
412	39	16.45	28	49.3	0.08	0.15	0.07	0.07	14.88	0.69	0.57	7
413	39	16.49	46	54.1	0.89	-0.32	0.17	0.16	15.92			0
414	39	16.65	21	10.8	0.47	0.08	0.22	0.16	15.83			1
415	39	16.78	28	1.9	0.05	0.05	0.05	0.03	14.12	0.78	0.77	93
416	39	16.94	38	32.4	-0.37	-0.61	0.13	0.05	14.72			0
417	39	17.19	31	59.0	-0.18	0.50	0.03	0.02	13.84			0
418	39	17.33	38	47.0	0.22	0.52	0.27	0.39	16.11	0.57	0.68	0
419	39	17.57	31	57.1	0.09	0.54	0.15	0.21	15.91	0.65	0.67	0
420	39	17.62	45	34.7	0.02	0.05	0.04	0.05	10.63	0.20	0.06	99
421	39	18.02	37	59.3	0.29	0.29	0.16	0.12	14.88	0.72	0.63	0
422	39	18.03	16	4.0	0.38	0.05	0.22	0.07	15.34	1.12	1.00	0
423	39	18.10	44	7.1	-0.22	0.04	0.23	0.17	15.28	0.91	0.85	1
424	39	18.21	24	26.2	0.02	0.03	0.15	0.25	15.93	1.08	1.37	46
425	39	18.67	36	21.7	0.04	0.02	0.05	0.03	15.02	1.08	1.15	75
426	39	18.80	24	24.5	0.75	0.32	0.40	0.28	16.28	0.73	0.69	0
427	39	19.41	47	48.9	-0.08	0.57	0.01	0.02	13.49			0
428	39	19.59	44	3.7	0.04	-0.15	0.21	0.28	15.91	0.67	0.64	45
429	39	19.65	18	32.9	1.18	-0.79	0.08	0.06	14.87			0
430	39	19.90	29	17.0	0.67	0.18	0.02	0.01	12.86			0
431	39	20.64	24	28.7	-0.11	0.22	0.18	0.31	15.91	0.14	0.27	14
432	39	20.64	47	34.7	0.39	0.58	0.12	0.27	15.17			0
433	39	21.00	23	38.1	-0.01	0.06	0.03	0.03	12.35	0.62	0.58	98
434	39	21.02	47	0.5	0.05	-0.04	0.02	0.02	13.62	0.51	0.38	97
435	39	21.05	32	6.8	-0.07	-0.08	0.01	0.02	11.45	0.34	0.28	97
436	39	21.67	30	7.6	0.15	0.04	0.21	0.15	15.88	0.79	0.75	37
437	39	21.72	17	12.3	0.89	0.06	0.30	0.41	15.63			0
438	39	21.80	23	17.7	0.16	0.60	0.06	0.08	14.63	0.49	0.36	0
439	39	21.87	43	7.8	-0.09	0.51	0.03	0.04	13.86			0
440	39	22.18	33	41.7	-0.11	0.00	0.24	0.13	15.44	0.71	0.65	43
441	39	22.31	31	10.8	0.69	0.23	0.08	0.07	14.69			0
442	39	22.48	19	28.1	-0.08	0.09	0.39	0.32	15.34	0.68	0.58	36
443	39	22.52	20	45.8	-0.39	0.27	0.20	0.20	15.93	0.76	0.92	0
444	39	22.54	41	47.5	0.45	0.29	0.10	0.07	15.08			0
445	39	22.61	24	46.0	0.11	0.46	0.14	0.23	15.16	0.58	0.48	0
446	39	22.69	28	14.7	-0.59	-0.41	0.02	0.02	13.68			0
447	39	22.92	42	5.0	-0.04	-0.01	0.05	0.07	10.42	0.14	0.10	99
448	39	22.96	21	29.4	-0.01	0.28	0.16	0.13	14.63	0.57	0.66	0
449	39	23.51	34	36.9	0.35	0.31	0.22	0.15	15.50	0.60	0.47	1
450	39	23.89	17	44.2	0.35	0.21	0.18	0.12	15.31			0
451	39	24.39	30	5.3	-0.06	0.03	0.02	0.03	12.33	0.50	0.47	98
452	39	24.43	48	44.8	0.99	-0.23	0.03	0.03	13.20			0
453	39	24.59	33	45.9	-0.16	0.15	0.02	0.02	13.71			0
454	39	25.41	37	3.1	0.10	-0.03	0.03	0.04	11.45	0.36	-1.02	99
455	39	25.58	20	58.0	-0.17	-0.05	0.07	0.07	15.29	0.55	0.55	11
456	39	25.84	23	8.1	8.02	-5.84	0.46	0.14	16.17			0
457	39	25.88	27	49.0	1.05	0.26	0.16	0.19	15.76			0
458	39	26.31	36	0.4	0.37	0.25	0.12	0.18	15.73	1.09	1.02	1
459	39	26.67	33	38.3	0.34	0.79	0.39	0.16	15.98	0.73	0.39	0
460	39	27.01	34	17.7	0.88	0.28	0.02	0.02	13.16			0
461	39	27.72	47	47.3	0.27	0.25	0.26	0.19	15.42	0.82	0.91	0
462	39	27.82	48	5.8	0.27	0.01	0.02	0.02	13.03	0.66	0.64	0
463	39	28.48	44	15.2	0.14	-0.10	0.03	0.04	11.95	0.58	0.48	55
464	39	28.99	47	51.6	-0.15	0.60	0.28	0.26	15.51	0.65	0.47	0
465	39	29.00	27	47.7	0.04	-0.01	0.02	0.01	12.84	0.57	0.58	99
466	39	29.40	27	30.3	1.25	0.42	0.12	0.06	14.60			0
467	39	29.48	29	5.5	0.43	0.40	0.15	0.14	15.10	0.42	0.51	0
468	39	29.57	29	34.0	-0.04	0.10	0.02	0.02	12.83	0.53	0.51	70
469	39	29.71	39	46.5	-0.01	-0.33	0.15	0.23	15.70	1.37	1.31	19
470	39	29.83	29	50.4	-0.02	-0.65	0.06	0.05	14.48	0.82	0.78	0
471	39	30.11	44	48.1	-0.09	0.18	0.04	0.05	14.32	0.44	0.40	0
472	39	30.27	18	35.9	-0.04	-0.09	0.03	0.05	14.20	0.59	0.51	68
473	39	30.42	28	17.0	0.02	0.00	0.21	0.23	15.28	0.64	0.68	78
474	39	31.11	36	43.0	-0.02	0.01	0.04	0.06	10.28	0.10	-0.50	99
475	39	31.17	23	37.4	0.34	0.02	0.29	0.30	16.19	1.12	1.32	10
476	39	31.17	27	14.8	1.76	0.62	0.20	0.17	15.59			0
477	39	31.22	37	59.9	-1.27	0.21	0.02	0.01	12.66			0
478	39	31.62	36	14.3	-0.05	0.01	0.27	0.29	16.10	0.51	0.67	45
479	39	31.64	28	40.8	-0.13	0.51	0.20	0.09	15.36	0.78	0.86	0
480	39	31.66	41	17.0	-0.96	-0.47	0.05	0.03	14.23			0
481	39	31.69	32	29.4	0.13	1.52	0.14	0.23	14.96			0
482	39	31.74	39	22.0	0.04	0.02	0.23	0.19	15.36	1.11	0.99	75
483	39	31.81	29	16.8	0.07	0.06	0.03	0.02	11.33	0.33	0.22	99
484	39	32.50	21	38.6	0.05	-0.04	0.07	0.03	12.25	0.53	0.50	98
485	39	32.56	39	40.1	0.29	0.07	0.23	0.18	15.91	0.79	0.65	15
486	39	32.65	47	56.5	-0.14	0.21	0.17	0.24	15.28			0
487	39	32.99	26	27.7	0.26	0.06	0.11	0.14	15.02	0.90	0.94	1
488	39	33.21	30	30.4	-0.02	0.00	0.02	0.02	12.78	0.58	0.52	99
489	39	34.11	34	59.5	-0.04	-0.06	0.17	0.11	15.00	0.95	0.96	67
490	39	34.15	21	49.0	0.01	-0.49	0.02	0.02	13.55			0
491	39	34.36	28	4.8	0.02	0.01	0.02	0.03	10.57	0.14	0.03	99
492	39	34.44	25	1.7	-0.40	0.21	0.04	0.03	14.35			0
493	39	34.54	35	25.2	0.77	0.17	0.17	0.21	15.13			0
494	39	34.75	33	49.3	-0.20	0.60	0.21	0.20	15.46	0.70	0.55	0
495	39	35.63	32	19.6	0.21	0.07	0.55	0.35	16.53	0.90	0.76	26
496	39	35.92	41	49.1	-0.15	0.29	0.07	0.05	14.56	0.93	0.85	0
497	39	36.37	32	19.9	0.03	0.23	0.65	0.32	16.46	0.82	0.62	18
498	39	36.80	26	15.1	0.58	0.05	0.21	0.20	15.71			0
499	39	36.88	45	24.5	0.48	0.38	0.09	0.07	14.88			0
500	39	36.88	31	38.0	0.64	0.87	0.22	0.16	15.58			0
501	39	37.19	38	59.4	0.02	0.64	0.26	0.35	15.67	0.71	0.61	0
502	39	37.41	22	10.7	0.06	0.06	0.04	0.03	11.23	0.33	0.23	99
503	39	37.72	35	9.2	0.01	-0.01	0.01	0.02	12.90	0.69	0.68	99
504	39	37.84	30	45.4	-0.08	0.05	0.01	0.03	11.75	0.44	0.37	97
505	39	38.08	33	5.1	-0.13	-0.02	0.07	0.06	14.76	0.62	0.48	36
506	39	38.21	30	15.8	0.35	0.51	0.22	0.28	16.11			0
507	39	38.41	21	29.0	1.09	0.21	0.01	0.03	12.26			0
508	39	38.55	39	53.8	0.71	0.36	0.19	0.15	15.43			0
509	39	38.82	43	53.5	0.13	0.34	0.23	0.18	15.08	0.95	0.87	0
510	39	38.88	29	49.5	-0.28	-0.24	0.36	0.12	16.23	1.06	1.27	8
511	39	39.35	21	9.5	0.20	0.08	0.03	0.03	11.69	0.36	0.25	23
512	39	40.26	31	22.8	0.39	0.67	0.19	0.16	15.06			0
513	39	40.61	24	54.9	-0.08	-0.05	0.07	0.05	14.47	0.96	1.00	39
514	39	41.02	39	44.9	-0.10	-0.46	0.29	0.25	16.16	0.75	0.73	3
515	39	41.12	28	27.6	0.02	0.04	0.02	0.01	13.28	0.63	0.60	98
516	39	41.47	33	7.3	0.10	0.16	0.13	0.19	15.98	1.06	1.29	27
517	39	42.28	29	29.5	-0.01	0.16	0.01	0.04	13.34	0.74	0.67	3
518	39	42.49	36	24.9	0.35	0.10	0.02	0.03	10.85			0
519	39	42.61	39	14.6	2.25	-0.14	0.35	0.25	16.28			0
520	39	43.08	21	32.9	-0.24	1.33	0.02	0.01	13.01			0
521	39	43.15	43	8.7	0.66	0.94	0.07	0.04	14.43			0
522	39	43.54	22	38.8	-0.25	-0.27	0.09	0.10	14.40	0.89	0.86	0
523	39	43.66	37	52.0	0.44	0.29	0.13	0.22	15.71			0
524	39	43.93	45	20.8	0.32	-0.12	0.15	0.17	14.85	0.94	0.89	0
525	39	43.95	24	58.2	0.24	-0.03	0.02	0.02	13.09	0.62	0.55	0
526	39	44.33	21	57.2	0.00	0.63	0.03	0.02	13.18			0
527	39	44.36	29	3.7	-0.25	-0.62	0.27	0.23	16.53			0
528	39	44.44	37	3.1	0.09	0.14	0.18	0.20	15.73			30
529	39	44.67	24	49.6	0.61	-0.07	0.07	0.07	15.16			0
530	39	44.84	44	55.5	0.29	0.55	0.22	0.36	16.22	0.96	0.96	0
531	39	44.92	46	40.5	-0.78	0.46	0.07	0.06	14.76			0
532	39	45.00	32	32.4	0.00	0.03	0.03	0.02	13.50	0.76	0.66	97
533	39	45.77	41	0.0	0.09	0.05	0.03	0.04	11.35			99
534	39	45.87	35	40.7	0.00	-0.17	0.29	0.29	15.80			43
535	39	45.99	21	9.6	0.29	0.06	0.05	0.03	13.92	0.54	0.52	0
536	39	46.04	45	18.6	0.08	-0.03	0.18	0.14	15.67	1.00	1.21	47
537	39	46.10	27	52.4	0.21	0.63	0.01	0.03	12.38			0
538	39	46.21	21	13.3	-0.06	0.27	0.39	0.29	15.49	0.64	0.55	0
539	39	46.26	20	31.4	0.00	0.33	0.21	0.13	15.69	1.09	1.19	6
540	39	46.49	46	32.9	-0.07	-0.02	0.27	0.27	15.41	0.61	0.69	63
541	39	46.56	22	19.2	0.46	0.35	0.22	0.10	15.22	0.64	0.65	0
542	39	46.64	39	41.6	-0.13	0.72	0.03	0.02	13.87			0
543	39	47.03	18	56.2	0.72	0.04	0.22	0.30	16.01			0
544	39	47.06	28	22.3	-0.43	0.27	0.11	0.09	14.70			0
545	39	47.06	40	57.2	-0.25	0.49	0.06	0.07	14.19			0
546	39	47.15	27	16.2	0.01	0.03	0.02	0.02	11.87	0.50	0.46	99
547	39	47.82	25	7.6	0.81	0.77	0.38	0.21	16.39	0.83	0.85	0
548	39	48.04	27	30.8	-0.02	0.00	0.02	0.02	12.91	0.58	0.55	99
549	39	48.19	25	52.8	0.31	0.04	0.04	0.09	15.22	0.98	0.97	0
550	39	48.53	19	29.3	2.22	-0.49	0.02	0.02	12.76			0
551	39	48.59	22	13.4	-0.09	0.68	0.36	0.13	15.63	0.60	0.62	0
552	39	48.77	34	59.7	-0.60	-0.05	0.02	0.02	12.94			0
553	39	48.77	21	49.1	0.62	0.39	0.21	0.11	15.25			0
554	39	49.79	39	11.7	-0.39	0.39	0.42	0.30	15.92			0
555	39	49.87	28	23.0	0.13	0.83	0.03	0.01	12.39			0
556	39	50.35	29	31.8	0.03	0.01	0.01	0.02	13.21	0.63	0.60	99
557	39	51.86	34	14.1	0.77	0.61	0.14	0.12	15.12			0
558	39	52.34	45	8.4	-0.03	0.72	0.23	0.29	15.52	0.48	0.65	0
559	39	53.37	19	34.5	0.20	0.28	0.04	0.05	14.13	0.59	0.59	0
560	39	53.54	41	53.2	0.03	0.35	0.18	0.29	15.82	1.23	1.13	4
561	39	53.58	35	4.2	0.13	0.70	0.03	0.02	12.65			0
562	39	53.74	44	10.2	0.35	0.02	0.17	0.15	15.01	0.75	0.72	0
563	39	54.43	41	49.5	-0.45	0.24	0.63	0.21	15.62	1.03	0.93	0
564	39	54.49	37	3.8	-0.44	0.87	0.08	0.08	14.20			0
565	39	54.75	21	44.2	0.41	0.14	0.10	0.05	14.48			0
566	39	55.75	22	47.3	-0.46	0.36	0.10	0.11	14.40			0
567	39	55.93	41	21.7	0.25	0.02	0.15	0.17	15.15	1.02	0.97	2
568	39	55.96	41	56.9	-0.01	0.63	0.17	0.15	14.98	0.60	0.40	0
569	39	56.19	34	2.8	0.36	0.06	0.05	0.06	14.64			0
570	39	56.40	41	50.5	-0.02	0.07	0.14	0.14	14.74	0.95	0.86	72
571	39	56.43	26	20.0	1.77	-2.22	0.14	0.12	14.92			0
572	39	56.59	23	39.8	0.25	0.49	0.02	0.03	13.25			0
573	39	56.61	21	49.0	-0.22	0.15	0.02	0.03	12.07			0
574	39	56.62	24	53.2	0.78	0.15	0.03	0.03	14.24			0
575	39	56.97	21	47.1	0.78	0.28	0.89	0.46	15.73			0
576	39	57.03	31	6.1	0.47	0.62	0.51	0.22	16.25			0
577	39	57.83	29	15.6	0.07	0.34	0.04	0.03	13.75			0
578	39	58.11	36	50.1	0.49	0.21	0.05	0.07	14.71			0
579	39	58.87	34	52.6	0.41	0.31	0.32	0.38	15.80			0
580	39	58.91	32	3.6	0.28	0.26	0.20	0.17	15.55			4
581	39	59.16	24	24.5	0.21	0.23	0.05	0.05	14.34			0
582	39	59.33	37	43.1	0.56	0.63	0.33	0.13	16.15			0
583	39	59.37	42	51.0	1.08	0.23	0.23	0.09	15.15			0
584	39	59.51	23	38.4	0.53	0.60	0.01	0.03	11.94			0
585	39	59.61	45	28.6	-2.58	-2.29	0.05	0.04	14.17			0
586	40	1.11	27	56.8	0.69	0.33	0.07	0.07	15.18			0
587	40	1.24	33	23.0	0.02	0.70	0.04	0.02	13.85			0
588	40	1.71	44	26.0	0.16	0.06	0.03	0.02	10.91			94
589	40	2.34	40	24.0	0.15	0.98	0.06	0.06	14.68	1.01	0.90	0
590	40	2.59	42	41.0	0.00	0.53	0.06	0.04	14.14	0.77	0.69	0
591	40	3.22	38	11.9	0.10	0.00	0.03	0.02	10.69			99
592	40	3.28	36	29.8	-0.13	-0.15	0.18	0.13	14.85	0.82	0.73	5
593	40	3.35	24	16.5	0.51	0.61	0.23	0.26	15.65			0
594	40	4.34	33	55.3	0.05	0.05	0.05	0.05	13.87	0.78	0.68	94
595	40	5.13	30	31.8	0.72	1.12	0.41	0.11	15.91			0
596	40	5.30	30	46.7	0.13	0.00	0.03	0.04	11.56			96
597	40	5.33	34	43.5	0.23	1.11	0.03	0.03	10.57	0.52	0.47	0
598	40	7.05	44	6.9	3.54	-1.39	0.25	0.15	15.37			0
599	40	7.19	41	2.2	1.05	0.36	0.03	0.02	13.28			0
600	40	7.38	36	14.5	0.04	-0.30	0.29	0.25	15.99			24

TABLE 5. (continued)

Id	2^h+ min	sec	$42°$+ ′	″	μ_x	μ_y	σ_x	σ_y	V	B−V	V−I	P
601	40	7.89	41	53.9	0.21	0.18	0.05	0.08	14.03	1.12	0.96	0
602	40	9.51	42	16.8	0.86	0.78	0.09	0.21	15.74			0
603	40	9.57	42	33.5	0.00	0.03	0.02	0.01	12.57	0.56	0.53	99
604	40	11.47	30	21.3	0.09	0.02	0.02	0.02	13.19	0.64	0.56	90
605	40	11.52	43	12.9	0.13	0.26	0.04	0.02	13.03			0
606	40	11.82	39	47.2	0.05	0.50	0.02	0.03	13.18	0.27	0.11	0
607	40	12.04	37	26.1	0.19	-0.15	0.15	0.30	15.57	0.65	0.68	32
608	40	12.20	39	38.1	0.46	0.31	0.48	0.28	16.20	0.83	0.67	0
609	40	13.17	33	4.5	0.08	0.31	0.19	0.12	15.56			7
610	40	13.34	35	55.4	1.76	-0.09	0.26	0.14	15.91			0
611	40	14.64	32	35.3	1.96	0.70	0.36	0.27	16.23			0
612	40	16.39	40	21.1	0.21	-0.07	0.18	0.14	14.88	0.93	0.95	2
613	40	16.62	38	4.0	-0.33	0.59	0.04	0.05	13.49			0
614	40	16.90	35	4.9	0.41	0.32	0.05	0.04	11.50			0
615	40	17.22	35	56.0	0.56	0.77	0.26	0.17	15.14			0
616	40	17.78	25	16.4	0.53	0.20	0.31	0.32	15.84			0
617	40	17.96	25	46.0	0.32	0.26	0.30	0.30	15.60	0.96	0.81	3
618	40	18.41	25	50.1	0.16	0.00	0.10	0.06	13.57	0.76	0.73	8
619	40	19.23	29	44.1	0.27	0.19	0.20	0.14	14.91	0.96	0.86	0
620	40	20.06	37	37.1	0.22	0.59	0.10	0.12	15.56			0
621	40	20.46	28	16.9	0.60	0.46	0.24	0.21	16.00			0
622	40	21.10	30	23.9	0.53	-0.74	0.10	0.08	12.69			0
623	40	21.98	33	0.6	0.59	0.16	0.16	0.21	15.68			0
624	40	22.24	35	39.6	1.27	-0.31	0.45	0.27	15.74			0
625	40	23.00	36	1.9	0.01	-0.09	0.08	0.08	13.99	0.80	0.69	89
626	40	23.50	27	59.3	0.67	0.72	0.11	0.28	16.03			0
627	40	24.16	29	43.8	0.39	0.71	0.21	0.24	15.49			0
628	40	24.72	28	3.5	0.46	0.47	0.25	0.22	15.23			0
629	40	25.27	34	13.5	-0.16	0.22	0.05	0.07	13.89			0
630	40	26.43	31	15.8	0.02	0.45	0.18	0.11	14.92			0

from the IS measures will be for a true epoch of 1975.75, the epoch of our positions. These reductions for position had a mean error of 0.05 arcseconds, testifying to both the precision of our positions and the IS measures. In Table 7, column 1 is the IS identification number, columns 2 to 5 are the equatorial coordinates, equator and equinox 1950, epoch 1975.75, columns 6 and 7 the V magnitude and $B-V$ color, followed by a v if determined by IS and a J if determined by Johnson (1954). The last column gives the IS membership probability.

3. DISCUSSION

3.1 Color–Magnitude Diagram, Distance, Reddening, and Metallicity

Figure 6 is a color–magnitude diagram for the cluster using our data. The top panel plots V vs $(V-I)_K$ and the bottom panel V vs $B-V$. The magnitudes and colors have not been corrected for interstellar extinction or reddening. For stars brighter than $V=14.0$, only stars with probabilities greater than 90% are plotted, for stars between 14.0 and 15.0 stars with probabilities greater than 40% are plotted, while for stars fainter than $V=15.0$, stars with probabilities greater than 5% are plotted. This means that there is little contamination of field stars for bright stars, while there is heavy contamination for faint stars, as is evident from the color–magnitude diagrams. The bright end of the main sequence is missing from Fig. 6, since these stars were too bright for measurement by us.

Canterna *et al.* (1979) obtained intermediate and narrow band ($uvby$ and Hβ) photometry of 42 stars in the vicinity of NGC 1039. They concluded that the reddening is moderate (E$(B-V)=0\overset{\mathrm{m}}{.}07$) and uniform across the cluster, that the metallicity is near solar, the true distance modulus is $8\overset{\mathrm{m}}{.}2$ corresponding to a distance of 440 pc. IS obtained a distance modulus of $8\overset{\mathrm{m}}{.}28$ (450 pc) by fitting a theoretical solar metallicity ZAMS (VandenBerg & Bridges 1984) to the middle and lower part of the NGC 1039 main sequence. Meynet *et al.* (1993) obtained an apparent distance modulus of 8.65 using the models of Schaller *et al.* (1992) and an adopted reddening of 0.10, which would give a true distance modulus of 8.35.

We have determined a distance by comparing our color magnitude of NGC 1039 to the ZAMS given in Meynet *et al.* (1993). Since we have observed to fainter magnitudes, we have a longer stretch of the main sequence for comparison. We dereddened the stars by 0.07 mag, and found an apparent distance modulus of 8.60, or a true distance modulus of 8.38, in excellent agreement with Meynet *et al.*

3.2 Age

The age of the cluster is critical for studies of the evolution of rotation, lithium abundance, and chromospheric activity in solar type stars. It seems likely that major evolutionary changes take place in these quantities in the time between the age of the Pleiades, $\sim 10^8$ yr, and the age of the Hyades, $\sim 8\times 10^8$ yr (Soderblom *et al.* 1993a, 1993b). Together with NGC 6475 ($d\sim 250$ pc, age~ 220 Myr; Prosser *et al.* 1995), M34 is one of the few moderately-rich, nearby clusters which are intermediate in age between Pleiades and the Hyades. Canterna *et al.* (1979) obtained an age of 500 Myr for M34 using the method of the brightest main sequence star given by Schlesinger (1969, 1972). IS obtained an age of 2.5×10^8 yr by fitting the theoretical isochrones of Maeder & Mermilliod (1981) to their data. Meynet *et al.* (1993) obtained an age of 1.8×10^8 yr.

We have redetermined the age of the cluster by comparing our observations supplemented with the observations of IS and Johnson (1954) to the theoretical isochrones of Meynet *et al.* (1993). It is obvious from Fig. 6 that there are significant scatter in our colors. To improve our $B-V$ colors, we transformed our $(V-I)_K$ colors to $B-V$ in the same manner as Soderblom *et al.* (1993a), and averaged the transformed $(V-I)_K$ colors with the observed $B-V$ colors. The rms difference between our transformed $B-V$ and observed $B-V$colors was 0.05 mag for stars brighter than $V=14$. Assuming an equal error contribution from both the observed and transformed colors would give a precision of 0.025 mag to the averaged $B-V$ colors. We supplemented our data with that of IS for stars brighter than $V=11.0$ which had photoelectric magnitudes and colors. We dereddened the $B-V$ colors by 0.07 mag and obtained absolute visual magnitudes assuming an apparent distance modulus of 8.60. Figure 7 plots the resulting M_v against $(B-V)_0$ and the isochrones from Meynet *et al.* (1993) for ages of 2.0 and 3.2×10^8 yr. From Fig. 7 it would appear the NGC 1039 has an age on the order of 200–250 Myr, slightly greater than that assigned by Meynet *et al.* The difference in age is almost entirely due to the difference in the assumed reddening.

3.3 Spatial Distribution and Luminosity Function

For dynamically relaxed clusters, higher mass stars should show a higher central concentration. Although there is much evidence to support such mass segregation (see, for example, Francic 1989), some clusters too young to be relaxed also show mass segregation (Jones & Walker 1988). IS provide some evidence that the lower mass stars in M34 have a wider

TABLE 6. Cross identifications.

JP	UV	Lv	Br	JP	UV	Lv	Br	JP	UV	Lv	Br	JP	UV	Lv	Br
6	51	175		179	122	292		320	184	364		484	242	462	144
10		183		182		293		323	186	367	105	488	243	465	146
11		189		183	121	293		325	185			490	245	466	
16		197		184	123	294		326	187	368		491	244	468	147
17	60	196	32	186	125	295	71	329	191	370	108	502	248	470	148
21	63	200		190	124	297		331	188	373		503	246	473	
22	64			191	126	300	74	332	189	372	109	504	247	474	149
27	67	206		200	130	303		336	190	376		507	250	475	
31	69			201	129			338	197	377	113	515	252	482	
35	71	209		206	131	304	75	343	195	381		517	254	484	
50	76	219		208	133	305		345	196	382		518	253	485	
51	75	220	41	209	138	307		346	199	384		520	255	486	
53	77	222		210	132	308		349	202			525	256	488	
56	78	224		211	135	309	78	352	200	385	118	526	259	489	
59	79	226	43	212	134			355	203	386		532	257	491	
65	80	231		213	136	311		362	204	390	120	533	258	492	
67	81	233		215	140		80	366		392		535	263	494	
69	83	234		216	142	313		373		397		537	262	493	
73	84	239		219	139	314	81	374	207	396	122	542	260		
76	85	240		222	137	318		375	205	398		545		496	
79		241		223	143			382	208	400		546	264	497	154
81	86	246		224		317		384	210			548	265	499	
84	87	247		230	145	320		385	209	401		550	267	500	
87	88	248	51	231	144	322	83	387	212	405		552	266	502	
89	89	249		236	146	321		394	211	406		555		503	
97	90	250	52	246	147	324	84	395	215			556	268	504	
99	92			249	148	325		400	213	408		559		508	
100	91	253	54	250	150			404	216	410	127	561	269	509	
101	94	252		251	149	326		408	217	417		564	270	510	
103	93	256		256	155	329	89	410	219	419		572	271	514	
110	98			257	154		88	417	220	422		573	272	513	
112	95			260	153	332		420	218	423		577	273	518	
114	96	260	57	270	157	336	91	427	221	426		584	275	521	
115	100	261	58	275	161	337	92	430	223	427		585	274		
121		263		277	159	338		433	225	430	133	587	277	523	
122	101	264		279	162		94	434	222	428		588	276	524	
124	102	267		280	163	341		435	224	429	132	591		527	
133	104			282	164	342		439		432		596	281		
137	106	269	61	285	165			446	228	436		597	280		162
140	105	270		287	167			447	226	437	135	599	282	532	
141	107			290	169	348	98	451	231	438	136	603	283	536	
146	109	276	63	292	168	349	97	452	229	440		604	287	541	
148	110	277		294	171	352		453	230	439		605	285	540	
149	111	280		296	173			454	232	442	137	606	286	544	
150	116	278	64	297	172	354	100	460	234	446		613	294	557	
153	114	282		301	175	357	102	462	233	448		614	296	559	
155	115	283		302	177	358	103	463	235		138	618	298	564	
156	112	284	65	303	179			465	236	450	139	622	300	569	
162		286		305	176	359	104	468	237			625		573	
164		289		307	178			471		453					
165	118	287		315	180	361		474	238	454	140				
177	120			319	181	365		483	241	458	142				

TABLE 7. UV members.

UV	2^h+ min	sec	42^o+ ′	″	V	B−V	t	P
4	36	31.08	28	34.7	11.86	0.51	v	70
6	36	34.85	49	22.5	12.84	1.65	v	46
7	36	35.83	46	1.0	9.33	0.94	v	71
8	36	38.24	39	58.2	12.27	1.03	v	49
10	36	39.26	25	6.4	13.20	0.72	v	57
15	36	46.32	38	1.0	13.15	1.05	v	52
16	36	46.63	37	12.8	12.64	0.96	v	41
33	37	9.56	16	18.5	9.02	0.12	v	69
38	37	14.43	42	17.1	12.11	0.92	v	61
48	37	25.07	38	44.0	11.19	1.40	v	81
52	37	27.88	41	9.5	12.86	0.91	v	79
61	37	38.35	48	47.7	12.84	1.68	v	83
62	37	38.15	43	44.0	11.40	0.63	v	88
68	37	44.55	51	11.7	12.83	1.43	v	44
70	37	45.59	39	28.1	9.64	0.03	J	72
74	37	51.39	45	52.0	10.61	0.47	v	71
82	37	57.89	27	53.6	9.37	-0.03	v	87
97	38	11.47	53	17.3	12.94	1.29	v	43
113	38	22.16	49	55.7	13.18	1.07	v	42
141	38	35.10	33	28.0	8.98	0.00	J	89
151	38	39.08	14	0.8	10.64	0.22	v	80
156	38	43.31	34	37.5	8.52	0.00	J	87
160	38	45.00	34	44.9	8.46	0.01	J	85
166	38	48.37	32	8.5	9.72	0.17	J	88
174	38	52.42	29	41.4	8.33	-0.01	J	84
192	38	59.52	32	4.5	9.93	0.12	J	90
193	38	59.98	33	55.6	8.80	0.06	J	86
194	38	59.80	29	12.5	7.94	0.00	J	87
198	39	0.83	39	14.2	9.30	0.05	J	81
206	39	8.65	32	52.0	8.85	0.03	J	81
214	39	13.75	32	44.7	9.31	0.05	J	88
240	39	32.08	36	29.5	8.26	0.01	J	80
249	39	38.50	24	3.0	10.28	0.14	J	89
251	39	39.34	21	9.4	11.82	0.36	v	68
278	40	3.22	38	11.9	10.63	0.07	v	87
279	40	2.03	17	54.5	13.05	0.54	v	55
288	40	11.89	33	41.0	9.56	0.06	J	86
289	40	11.34	19	29.3	11.57	0.29	v	45
292	40	16.33	50	43.4	13.00	0.36	v	52
299	40	18.87	24	36.4	8.89	-0.02	J	89
309	40	30.38	33	42.5	13.15	1.18	v	63
310	40	32.45	33	52.5	12.42	0.49	v	70
311	40	33.77	47	17.5	13.24	0.51	v	40
323	40	44.27	29	16.0	13.10	1.04	v	66
324	40	45.89	34	42.0	11.53	0.40	v	40
326	40	48.11	17	29.2	12.66	0.33	v	50
331	41	0.90	44	45.6	11.49	0.29	v	53
340	41	9.16	36	43.5	12.61	0.71	v	45

distribution than the higher mass stars. However, one must use some caution when using membership probabilities to determine spatial distribution when the parameters do not have a magnitude dependence. In general in such determinations, there will be a greater contamination of nonmembers

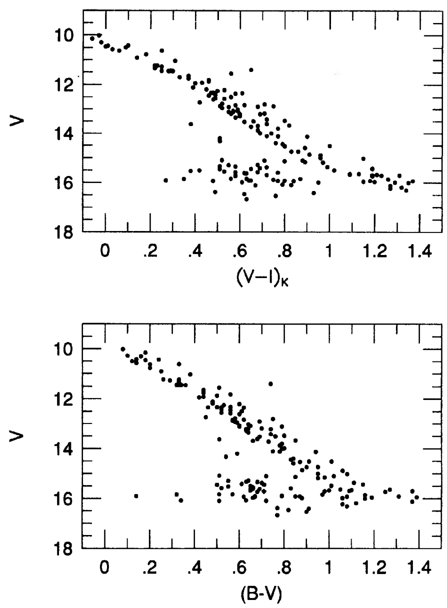

FIG. 6. The color magnitude for M34 in $B-V$ (bottom) and $(V-I)_K$ (top) using our data. Stars with probabilities greater than 90% are plotted for stars brighter than $V=14$, greater than 40% for stars between 14 and 15, and greater than 5% for stars fainter than 15.

for the fainter stars, and this will lead one to conclude that the distribution of faint members is wider than is actually the case.

With an assumed projected surface density of the form $\rho(r)=\rho_0 \exp(r/r_0)$, where r_0 is the scale length for the projected surface density of cluster members, our values of r_0 determined from the probability solutions give a measure of the concentration of the cluster. In principle r_0 could be used to determine, magnitude by magnitude, how many cluster

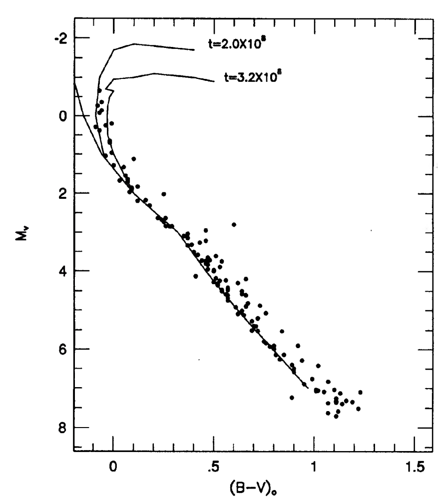

FIG. 7. A plot of M_v vs $(B-V)_0$ for a reddening of 0.07 mag and an apparent distance modulus of 8.60 mag. We have not plotted stars that fall significantly below the main sequence. We used the data of IS for the brighter stars ($V<11$) for which we had no data. The IS membership had to be greater than 80%. The isochrones are from Meynet *et al.* (1993).

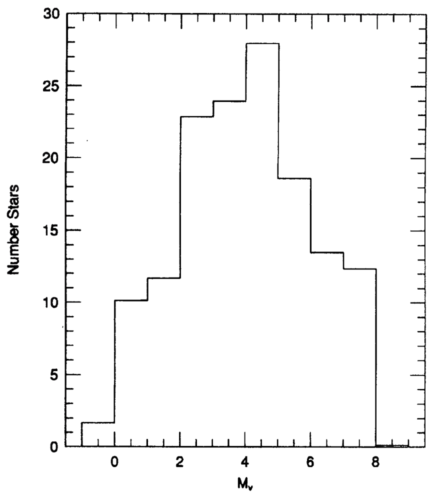

FIG. 8. The luminosity function of NGC 1039. The downturn faintward of M_v=4 is probably not real.

members are outside of our measuring area. Contrary to expectations, the values of r_0 do not increase to fainter magnitudes, but decrease or remain constant, although the errors are large. We are not in contradiction to IS's tentative conclusion that the fainter stars have a wider distribution, however, because their conclusion was based on stars brighter than $V=11$ compared to those fainter than $V=11$, and we have too few stars brighter than $V=11$ to make a sound conclusion.

We have combined our data with that of IS to produce a tentative luminosity function for the cluster. We summed our membership probabilities in one magnitude bins. We then looked at the IS stars that were within our measuring area. If the IS star was not in common with us, we added the IS probability to the sum in the appropriate magnitude bin. For the fainter stars, the additional stars added by IS were quite small because most stars were in common, while at the extreme bright end the stars are all IS stars. The resulting luminosity function is given in Fig. 8.

There is interest in cluster luminosity functions both as to what they can reveal regarding the universality of the initial mass function and also cluster dynamical evolution. However, we urge extreme caution in interpreting the luminosity function presented in Fig. 8 because of the problems discussed above. In particular the downturn for stars fainter than M_v=4 is most likely artificial because the luminosity function refers to the central projected four parsecs of the cluster.

We would like to thank Dr. Kyle Cudworth of Yerkes Observatory for generously allowing us to use the first epoch Yerkes plates and to Matt Shetrone and Debra Fischer for providing the radial velocities in advance of publication. This research was supported by the National Science Foundation under Grant No. NSF AST-9218084.

REFERENCES

Brüggemann, H. 1937. Astron. Abh. Hamburg. 4, 7
Canterna, R., Perry, C. L., & Crawford, D. L. 1979, PASP, 91, 263
Dieckvoss, W. 1955, Astron. Nach., 282, 25
Francic, S. P. 1989, AJ, 98, 888
Ianna, P. A., & Schlemmer, D. M. 1993, AJ, 105, 209 (IS)
Johnson, H. L. 1954, ApJ, 119, 185
Jones, B. F., Shetrone, M., & Fischer, D. 1995, private communication
Jones, B. F., & Stauffer, J. R. 1991, AJ, 102, 1080
Jones, B. F., & Walker, M. F. 1988, AJ, 95, 1755
Klemola, A. R, Jones, B. F., & Hanson, R. B. 1987, AJ, 94, 501
Latypov, A. A. 1973, Circ. Obs. Tashkent, No. 388
Maeder, A., & Mermilliod, J. C. 1981, A&A, 93, 136
Meynet, G., Mermilliod, J.-C., & Maeder, A. 1993, A&AS, 98, 477
Prosser, C. F., Stauffer, J. R., Caillault, J.-P., Balachandran, S., Stern, R. A., & Randich, S. 1995, AJ, 110, 1229
Sanders, W. L. 1971, A&A, 14, 226
Schaller, G., Schaerer, D., Meynet, G., & Maeder 1992, A&AS, 96, 269
Schlesinger, B. M. 1969, ApJ, 157, 533
Schlesinger, B. M. 1972, AJ, 77, 584
Soderblom, D. R., Jones, B. F., Balachandran, S., Stauffer, J. R., Duncan, D. K., Fedele, S. B., & Hudon, J. D. 1993a, AJ, 106, 1059
Soderblom, D. R., Stauffer, J. R., Hudon, J. D., and Jones, B. F. 1993b, ApJS, 85, 315
Vandenberg, D. A., & Bridges, T. J. 1984, ApJ, 278, 679